ISSN 1063-7710, Acoustical Physics, 2009, Vol. 55, No. 1, pp. 27–54. © Pleiades Publishing, Ltd., 2009.

NONLINEAR ACOUSTICS

Nonlinear Standing Waves, Resonance Phenomena, and Frequency Characteristics of Distributed Systems

O. V. Rudenko

Faculty of Physics, Moscow State University, Moscow, 191992 Russia
e-mail: rudenko@acs366.phys.msu.ru

Received August 26, 2008

Abstract—This review is dedicated to resonator oscillations under conditions of a strongly expressed nonlinearity under which steep shock fronts emerge in the wave profiles. Models and approximated methods for their analysis for quadratic and cubic nonlinear media are examined, as well as for nonlinearity when taking into account the mobility of boundaries. The forms of the profiles are calculated both for a steady-state oscillation regime and during the establishment of the profiles. Dissipative losses and selective losses at specially chosen frequencies are considered. An analysis of nonlinear Q-factor is given. The possibility of increasing the acoustic energy accumulated in the cavity of the resonator is discussed. Special attention is given to various physical phenomena that are exhibited only in nonlinear acoustic fields.

PACS numbers: 43.25.+y, 43.20.Ks, 43.25.Gf

DOI: 10.1134/S1063771009010047

INTRODUCTION

Resonance is one of the most interesting and fundamental phenomena in the physics of oscillations and waves. Resonance manifests itself clearly when the dependence of the amplitude of induced oscillations on frequency (frequency response of the system) has a sharp maximum. In these cases, the ratio of the central frequency ω_0 of the spectral line, representing a response, to the characteristic width of this line is a large value. This ratio, called the quality- or Q-factor, is used as a quality measure of the resonance system. At larger values of Q, the system may contain a high energy density, since the ratio of the amplitude of induced oscillations to the amplitude of oscillations of the external source providing an influx of energy to the system is also equal to Q. In hi-Q systems, approaching a state of equilibrium is a slow process with a characteristic relaxation time on the order of Q/ω_0. The time of the growth of oscillations (or their decay after the source is switched off) occurs over the course of many periods, the number of which is ~Q. Excitation of strong oscillations during resonance may lead to the appearance of nonlinear effects, the most well-known of which is destruction of the system. However, hi-Q systems are used for taking high-precision physical measurements.

The problem of increasing the quality of acoustic resonators is topical for many areas of physics and engineering. In distributed hi-Q systems, it is possible to accumulate significant energy and to create conditions for observing strongly expressed nonlinear effects even with weak pumping [1]. High-accuracy measurement systems used, in particular, for detecting hits of gravitational radiation [2] contain mechanical resonators made of sapphire and silicon, the quality of which has attained record values of 10^9 for sound frequency ranges at liquid helium temperatures [3]. The minimization of all possible losses (by means of growing perfect crystals, intensive polishing of faces, etc.) has made it possible even at room temperature to achieve values of $Q \sim 10^8$ (the corresponding time of relaxation is on the order of three years [4]). In such hi-Q systems, when linear (amplitude-independent) losses are almost completely excluded, nonlinear absorption can play the role of a limiting factor.

Nonlinearity is the main reason that Q is limited in less perfect resonators, but in the presence of intensive pumping. In such situations, foremost is the problem of suppressing nonlinear distortions of the wave profile, leading to the emergence of steep shock fronts, since it is mainly at the fronts where absorption occurs, independently of the dissipating characteristics of the medium [1]. There are at least three known methods for suppressing the emergence of a shock front.

In [5], a method was proposed for artificially introducing detunings between harmonics in the resonator, one of the walls of which possesses frequency-dependent impedance. Detunings between rigidly phased harmonics, which make up the shock front, "extend" (widen) it and decrease nonlinear losses.

In [6–8], the idea has been implemented of controlling a wave profile and phase shifts between harmonics at the expense of using resonators of complex form—conical, bulb-shaped, etc. With this method, it was possible to obtain, in gas-filled volumes, positive excess pressure in certain atmospheres and to achieve suppres-

sion of shock fronts under strong nonlinearity (for relatively large acoustic Mach numbers).

The third method is based on introducing selected absorbers into the medium. Generally speaking, the idea in [9] of suppressing "key" harmonics, the presence of which leads to uncontrolled diffluence of the wave energy across the spectrum, makes it possible to control energy flows and, in particular, to concentrate energy in the necessary harmonic components. An array of possibilities for controlling wave interactions, described in [10], can be used to increase the quality of a nonlinear acoustic resonator. In experiment [11], for instance, there was an increase in quality linked to the fact that one of the boundaries partially let the second harmonic outside, reflecting the wave of the main frequency inward. Thus, to increase Q, losses on the wavelength of the second harmonic were artificially introduced.

Therefore, methods exist for suppressing both linear and nonlinear losses in a resonator, which lead to an increase in quality.

METHOD FOR CALCULATING THE CHARACTERISTICS OF NONLINEAR RESONATORS

It is obvious that a standing wave in a one-dimensional linear resonator can be represented in the form of two waves traveling toward each other. This idea was generalized for nonlinear waves localized between two parallel rigid walls [12]; oscillations are described by the sum of counterpropagating Riemann and Burgers waves. Each of these waves can be strongly distorted due to nonlinear self-action, which transforms the initial harmonic profile into a profile of saw-tooth form; however, "cross" action appears to be extremely weak. In other words, each of the two opposing waves is distorted in and of itself in the process of propagation, but there is almost no energy exchange between them. A similar approach has been used [13] to describe a nonlinear field in a flat waveguide, where nonlinear Brillouin modes form as two nonacting—between themselves—strongly distorted waves traveling under the same angles toward the axis of the waveguide. This idea is not very obvious, but it can easily be explained.

The explanation given below is correct for any nonlinear equation describing nondispersive waves in a quadratic nonlinear medium. For certainty, we examine a very simple model equation [14]:

$$\frac{\partial^2 p}{\partial x^2} - \frac{1}{c^2}\frac{\partial^2 p}{\partial t^2} = -\frac{\varepsilon}{c^4\rho}\frac{\partial^2 p^2}{\partial t^2}. \quad (1)$$

Here, p is acoustic pressure, c and ρ are the speed of sound and the density of the medium, and ε is the nonlinearity parameter. Equation (1) can describe both Riemann waves traveling in opposite directions, and the interaction between them. We seek a weakly nonlinear solution by the method of successive approximations:

$$p = p^{(1)} + p^{(2)} + \ldots. \quad (2)$$

Let in the first approximation the solution describe two counterpropagating harmonic waves:

$$p^{(1)} = B_1\cos(\omega_1 t - k_1 x + \varphi_1) + B_2\cos(\omega_2 t + k_2 x + \varphi_2), \quad k_{1,2} = \omega_{1,2}/c. \quad (3)$$

The second approximation is found from the linear heterogeneous equation

$$\frac{\partial^2 p^{(2)}}{\partial x^2} - \frac{1}{c^2}\frac{\partial^2 p^{(2)}}{\partial t^2} = F(2\omega_1) + F(2\omega_2) + F(\omega_1 + \omega_2) + F(\omega_1 - \omega_2), \quad (4)$$

the right-hand side of which is calculated on the basis of the first approximation (3):

$$F(2\omega_{1,2}) = \frac{2\varepsilon}{c^4\rho}\omega_{1,2}^2 B_{1,2}^2\cos[2(\omega_{1,2}t \mp k_{1,2}x + \varphi_{1,2})],$$

$$F(\omega_1 \pm \omega_2) = \frac{\varepsilon}{c^4\rho}(\omega_1 \pm \omega_2)^2 B_1 B_2 \times \cos[(\omega_1 \pm \omega_2)t - (k_1 \mp k_2)x + (\varphi_1 \pm \varphi_2)]. \quad (5)$$

Using method (2), we can examine the four terms in the right-hand side of Eq. (4) as "external forces" exciting an "induced wave" of the second approximation at frequencies of the second harmonic of $2\omega_1$, $2\omega_2$, as well as the sum $(\omega_1 + \omega_2)$ and difference $(\omega_1 - \omega_2)$ frequencies.

It is important that excitation of secondary waves can have a resonance or nonresonance character. The first two forces of (5) $F(2\omega_1)$ and $F(2\omega_2)$ lead to resonance excitation. The corresponding induced waves

$$p_{1,2}^{(2)} = -\frac{\varepsilon}{2c^2\rho}B_{1,2}^2(\omega_{1,2}t) \times \sin[2(\omega_{1,2}t \mp k_{1,2}x + \varphi_{1,2})] \quad (6)$$

accumulate with time. Their amplitudes grow linearly with an increase in t similar to the amplitude of induced oscillations of a pendulum when of the eigenfrequency and the frequency of the inducing force coincide.

In contrast to concentrated systems, resonance in distributed systems occurs when the phase rates of motion of the inducing force and the wave proper coincide [14].

In contrast to waves (6), the amplitudes of which grow with an increase in t, partial solutions to Eq. (4),

which correspond to two different inducing forces $F(\omega_1 \pm \omega_2)$ in (5),

$$p_{3,4}^{(2)} = \frac{\varepsilon}{c^4\rho}\frac{(\omega_1 \pm \omega_2)^2}{4k_1k_2}B_1B_2 \times \cos[(\omega_1 \pm \omega_2)t - (k_1 \mp k_2)x + (\varphi_1 \pm \varphi_2)], \quad (7)$$

have amplitudes independent of time t.

Comparison of resonance (6) and nonresonance (7) solutions shows that after several periods of oscillations $(\omega_{1,2}t) \gg 1$, waves (7) seem much weaker in comparison to resonance waves (6) and therefore they cannot effectively participate in nonlinear energy exchange. Therefore, each of the two opposing waves generates its own high harmonics (6), but it is possible to neglect processes of cross interaction (7) if the waves oscillate with time. This conclusion is also correct for periodic waves that intersect at quite large angles (the values of the latter are determined by the acoustic Mach numbers [13]).

We switch now to the deduction of simplified equations, first taking into account only the quadratic nonlinearity of the medium. Let the left boundary $x = 0$ of the layer oscillate according to the law

$$u(x = 0, t) = Af(\omega t), \quad (8)$$

where A is the characteristic amplitude, u is the velocity, and f is the periodic function with a period of 2π. The right boundary $x = L$ is immobile:

$$u(x = L, t) = 0. \quad (9)$$

Using the method of a slowly changing profile [1, 14] and the correlation $p = \pm\rho cu$, linking the linear waves of pressure and vibration velocity, we combine the second-order nonlinear equation (1) with a pair of first-order equations for traveling Riemann waves:

$$\frac{\partial u}{\partial x} \pm \frac{1}{c}\frac{\partial u}{\partial t} - \frac{\varepsilon}{c^2}u\frac{\partial u}{\partial t} = 0. \quad (10)$$

Here the plus sign corresponds to a wave traveling to the right along the x axis, and the minus sign, to a wave traveling in the opposite direction. The sum of the two solutions is written as follows:

$$u = F\left[\omega t - \frac{\omega}{c}(x - L) + \frac{\varepsilon}{c^2}\omega(x - L)F\right] - F\left[\omega t + \frac{\omega}{c}(x - L) - \frac{\varepsilon}{c^2}\omega(x - L)F\right], \quad (11)$$

where F is an arbitrary function describing the profiles of nonlinear traveling waves. It is clear that solution (11) satisfies boundary condition (9). The second condition (8) transforms (11) into a functional equation relative to unknown F:

$$F\left[\omega t + kL - \frac{\varepsilon}{c}kLF\right] - F\left[\omega t - kL + \frac{\varepsilon}{c}kLF\right] = Af(\omega t). \quad (12)$$

An equation of type (12) is complex and cannot be solved analytically. In order to understand in general terms what information is contained in (12), we first exam a very simple case, supposing nonlinearity equal to zero, $\varepsilon = 0$, and boundary oscillations being harmonic: $f = \sin(\omega t)$,

$$F(\omega t + kL) - F(\omega t - kL) = A\sin(\omega t). \quad (13)$$

The solution to Eq. (13),

$$F = -\frac{A\cos(\omega t)}{2\sin(kL)} + \sum_{n=0}^{\infty}[A_n\cos(n\omega_0 t) + B_n\sin(n\omega_0 t)], \quad (14)$$

is the sum of the partial solution of inhomogeneous equation (13) and of the general solution to the corresponding homogeneous equation. Here,

$$\omega_0 = \pi c/L, \quad L = \lambda_0/2 \quad (15)$$

is the frequency of the main resonance. If the oscillation frequency of the boundary approaches one of the eigenfrequencies, $\omega \longrightarrow n\omega_0$, non-steady-state resonance growth begins. In order to demonstrate this, we put into solution (14)

$$A_m = \frac{A}{2\sin(kL)}, \quad B_n = 0, \quad A_n = 0 \ (n \neq m). \quad (16)$$

Solution (14), taking into account (16), contains an uncertainty of the type (0/0). Expanding it, we obtain

$$F = \frac{A}{2}\lim_{\omega \to n\omega_0}\frac{\cos(n\omega_0 t) - \cos(\omega t)}{\sin(\omega L/c)} = \frac{A}{2\pi}(-1)^n(\omega_0 t)\sin(n\omega_0 t). \quad (17)$$

Expression (17) describes a resonance oscillation with increasing amplitude. This simple example illustrates the unobvious, at first glance, fact that functional equations of type (12), (13) describe not only steady-state oscillations, but also various transition processes.

We proceed now to nonlinear functional equation (12). It can be reduced to a simplified evolutionary equation in satisfying a number of conditions. First, the length of the resonator should be small in comparison to the characteristic nonlinear length. Second, the boundary oscillation frequency of the resonator should not greatly dif-

fer from the eigenfrequencies (for instance, the frequencies of the main mode):

$$L \ll \frac{c^2}{\varepsilon\omega F_{\max}}, \quad kL = \pi + \Delta, \qquad \Delta = \pi\frac{\omega - \omega_0}{\omega_0} \ll 1. \tag{18}$$

Here, $F_{\max}$ is the maximal value of function F, and Δ is a dimensionless detuning frequency. Taking into account (18), the right-hand side of Eq. (12) can be expanded in a series:

$$F\left[\omega t + \pi + \Delta - \pi\frac{\varepsilon}{c}F\right] - F\left[\omega t - \pi - \Delta + \pi\frac{\varepsilon}{c}F\right] \approx [F(\omega t + \pi) - F(\omega t - \pi)] + \left(\Delta - \pi\frac{\varepsilon}{c}F\right)[F'(\omega t + \pi) + F'(\omega t - \pi)]. \tag{19}$$

It is obvious that F is an almost periodic function with parameters that slowly change with time. Therefore,

$$F(\omega t + \pi) - F(\omega t - \pi) \approx 2\pi\mu\frac{\partial F}{\partial(\mu\omega t)}, \tag{20}$$

where $\mu \ll 1$ is a small parameter whose the physical sense is explained below. Equation (12) now takes the form

$$\mu\frac{\partial F}{\partial(\mu\omega t/\pi)} + \left(\Delta - \pi\frac{\varepsilon}{c}F\right)\frac{\partial F(\omega t + \pi)}{\partial(\omega t)} = \frac{A}{2}f(\omega t). \tag{21}$$

Introducing new dimensionless variables and constants,

$$\xi = \omega t + \pi, \quad U = F/c, \quad M = A/c, \quad T = \omega t/\pi, \tag{22}$$

we rewrite (21) as follows:

$$\frac{\partial U}{\partial T} + \Delta\frac{\partial U}{\partial \xi} - \pi\varepsilon U\frac{\partial U}{\partial \xi} = \frac{M}{2}f(\xi - \pi). \tag{23}$$

It is now clear that small parameter μ has a value on the order of the small numbers: Δ, M, and $U \sim M$.

In [15, 16], an equation was obtained that generalizes (23). Namely, the effects of linear dissipation and the finiteness of displacement of a mobile boundary were taken into account. This equation is deduced by analogous means and has the form

$$\frac{\partial U}{\partial T} - M\Phi(\xi)\frac{\partial U}{\partial \xi} + \Delta\frac{\partial U}{\partial \xi} - \pi\varepsilon U\frac{\partial U}{\partial \xi} - D\frac{\partial^2 U}{\partial \xi^2} = \frac{M}{2}\Phi'(\xi), \tag{24}$$

where $\Phi(\xi)$ is a periodic function and

$$D = \frac{b\omega^2}{2c^3\rho}L \ll 1 \tag{25}$$

is a dimensionless dissipative parameter that determines weak absorption of waves passing one resonator length L, and b is the effective viscosity of the medium [1, 14].

STANDING WAVES AND THE Q-FACTOR OF A RESONATOR FILLED WITH A DISSIPATIVE MEDIUM

In considering quadratic nonlinearity and dissipation conditioned by the effects of viscosity and thermal conductivity of the medium, each of the two counterpropagating nonlinear waves is described by an equation that follows from (23), (24):

$$\frac{\partial U}{\partial T} + \Delta\frac{\partial U}{\partial \xi} - \pi\varepsilon U\frac{\partial U}{\partial \xi} - D\frac{\partial^2 U}{\partial \xi^2} = \frac{M}{2}f(\xi - \pi). \tag{26}$$

Equation (26) is known as the inhomogeneous Burgers equation with detuning [17]. Its main properties have been studied in [17–19]. The non-steady-state solution to Eq. (26) can be found in the most interesting resonance case ($\Delta = 0$) for certain special forms of boundary oscillations. These exact solutions can help in understanding the general properties of induced nonlinear oscillations of resonators.

Let the boundary perform periodic saw-tooth movements. In one period, the form of oscillations is given by the expression

$$f(\omega t) = \left(1 - \frac{\omega t}{\pi}\right)\mathrm{sgn}(\omega t), \quad -\pi \le \omega t \le \pi. \tag{27}$$

We seek the solution to (26), (27) in the form

$$U = -a(T)\xi/\pi, \quad f = -\xi/\pi, \quad -\pi \le \xi \le \pi. \tag{28}$$

For the "saw amplitudes" we obtain a ordinary differential equation and corresponding solution,

$$\frac{da}{dT} + \varepsilon a^2 = \frac{M}{2}, \quad a = \sqrt{\frac{M}{2\varepsilon}}\tanh\left(\sqrt{\frac{\varepsilon M}{2}}T\right). \tag{29}$$

We see that the amplitude increases with time, tending, at $T \longrightarrow \infty$, toward the maximum value $(M/2\varepsilon)^{1/2}$.

The form of a standing wave is described by solution (11), in which it is possible to ignore the nonlinear term if oscillations are examined within one period. As well, (11) takes the simple form

$$u/c = U(\omega t - kx) - U(\omega t + kx). \tag{30}$$

The time profiles of a standing wave described by formulas (28)–(30) are constructed in Fig. 1 for various sections of the resonator situated at $x = L/8$, $L/4$, $L/2$, $3L/4$, and $7L/8$. We see that the form of the velocity of induced nonlinear oscillations changes in the transition from one cross section to another. In the middle of the

layer, each period consists of alternating areas of positive and negative polarity of the same rectangular shape. Upon approaching the end of $x = L$, the area of positive polarity converges, but its "height" grows, right up to a value twice that of the middle section, $x = L/2$. The area of negative polarity decreases in value, but stretches along the time axis. The entire area under the curve (the integral from u over the period) is equal to zero.

Upon approaching the other boundary, $x = 0$, convergence with time and growth in amplitude of the area of negative polarity occur. At both boundaries, $x = 0$ and L, movement disappears and $u = 0$, in accordance with boundary conditions (8), (9). For a mobile boundary, satisfaction of condition (8) need not be taken literally; it is necessary to bear in mind that the amplitude of wall oscillations is very small in comparison to the characteristic amplitude of field u oscillations in the cavity of the resonator.

The mean volume density of energy for the period,

$$\rho\overline{u^2} = \frac{\rho}{2\pi}\int_0^{2\pi} u^2 d(\omega\tau) = \rho c^2 8kx\left(1 - \frac{kx}{\pi}\right)a^2(T), \quad (31)$$

has a maximum at the center of the layer, $kx = \pi/2$, and is equal to zero at both boundaries. The full energy in volume V of the resonator, calculated with integration of (31) by coordinate, is

$$E = \frac{1}{3}\rho c^2 V \frac{M}{\varepsilon}\tanh^2\left(\sqrt{\frac{\varepsilon M}{2}}\frac{\omega t}{\pi}\right). \quad (32)$$

The ratio of the amplitude of a standing wave and boundary oscillations increases with an increase in time,

$$Q = \frac{a(T)}{M} = \frac{1}{\sqrt{2\varepsilon M}}\tanh\left(\sqrt{2\varepsilon M}\frac{\omega t}{2\pi}\right), \quad (33)$$

achieving the maximal value having the sense of a steady-state nonlinear Q-factor:

$$Q_{NL} = \sqrt{c/2\varepsilon A}. \quad (34)$$

We see that the Q-factor drops with an increase in amplitude A of boundary oscillations. If the nonlinearity is very small, the Q-factor does not depend on amplitude A and is determined by regular linear absorption (see, for instance, [16]):

$$Q_{LIN} = \frac{1}{2D} = \frac{c^3\rho}{b\omega^2 L} = \frac{c^2\rho}{\pi b\omega}. \quad (35)$$

In contrast to nonlinear Q-factor (34), linear Q-factor (35) is fully determined by the resonator geometry and the properties of the medium it is filled with. For an amplitude of boundary oscillations of $A = 10$ cm/s, the nonlinear Q-factor of an air resonator is $Q_{NL} \approx 40$. On the other hand, for typical frequency values on the order of 4 kHz, the linear Q-factor is much higher, on the order of 10^3–10^4. However, when there is a high linear Q-factor, the amplitude of a standing wave grows with time; the conditions for manifestation of nonlinear effects become even more favorable, and nonlinear absorption can lead to a significant drop in Q-factor.

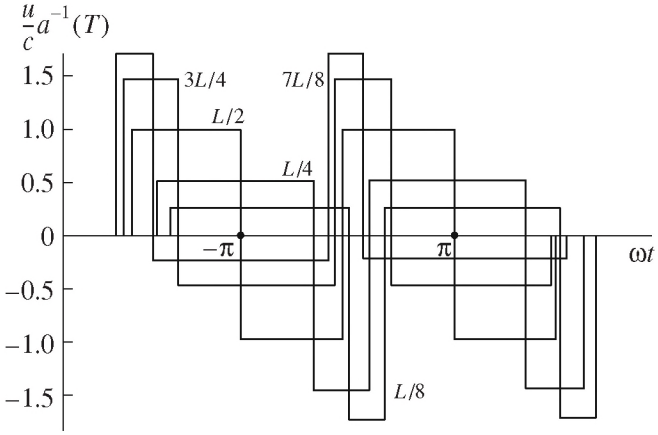

Fig. 1. Profiles of the standing wave described by Eqs. (28)–(30), constructed in various sections of the resonator: $x = L/8, L/4, L/2, 3L/4, 7L/8$.

For the harmonic law of wall oscillations, the right-hand side of the Eq. (26) has the form $-(M/2)\sin\xi$. In this and certain other cases, the inhomogeneous Burgers equation is solved with the help of linearization. Using the transformation

$$U = \frac{2D}{\pi\varepsilon}\frac{\partial}{\partial\xi}\ln W, \quad (36)$$

it is possible to reduce Eq. (26) to the following linear equation:

$$\frac{\partial W}{\partial T} + \Delta\frac{\partial W}{\partial\xi} - D\frac{\partial^2 W}{\partial\xi^2} = \frac{1}{2}qD\cos\xi W, \quad q = \frac{\pi\varepsilon M}{2D^2}. \quad (37)$$

Yet another substitution

$$W = \exp(-\lambda DT/4)y(z = \xi/2), \quad (38)$$

where λ is a constant, combine (37) with the ordinary differential equation for function $y(z)$:

$$\frac{d^2 y}{dz^2} - 2\frac{\Delta}{D}\frac{dy}{dz} + (\lambda + 2q\cos 2z)y = 0. \quad (39)$$

At zero detuning, $\Delta = 0$, Eq. (39) is it the canonical form of the differential equation for the Mathieu function [20]. Namely, the resonance ($\Delta = 0$) case admits a full analytical study.

For the zero initial condition $U(T = 0, \xi) = 0$, the solution to Eq. (37) is written in the form of a series of even Mathieu functions:

$$W = \sum_{n=0}^{\infty} a_{2n}\exp\left[-\frac{1}{4}\lambda_{2n}(q)DT\right]ce_{2n}\left(\frac{\xi}{2}, q\right), \quad (40)$$

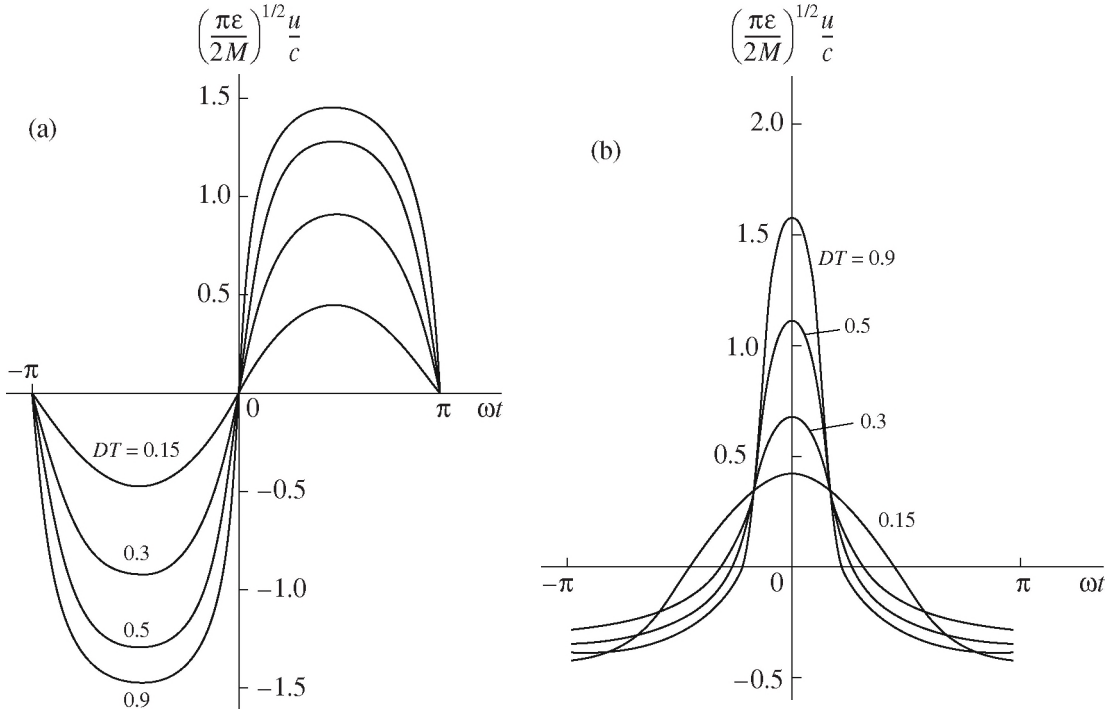

Fig. 2. Process of a standing wave being established during harmonic boundary oscillations in the midsection of the resonator $x = L/2$ (a) and near the right end face $x = 7L/8$ (b). The value of slow time $DT = 0.15, 0.3, 0.5, 0.9$. Parameter $q = 20$.

where the coefficients are determined by the formulas

$$a_{2n} = \left[\int_0^{2\pi} ce_0\left(\frac{\xi}{2}, q\right)d\xi\right] \Big/ \left[\int_0^{2\pi} ce_{2n}^2\left(\frac{\xi}{2}, q\right)d\xi\right]. \quad (41)$$

The notations used here correspond to [20].

A simple formula is obtained for the steady-state (at $T \longrightarrow \infty$) profile of a wave [18].

$$U = \frac{2D}{\pi\varepsilon}\frac{d}{d\xi}\ln ce_0\left(\frac{\xi}{2}, q = \frac{\pi\varepsilon M}{2D^2}\right). \quad (42)$$

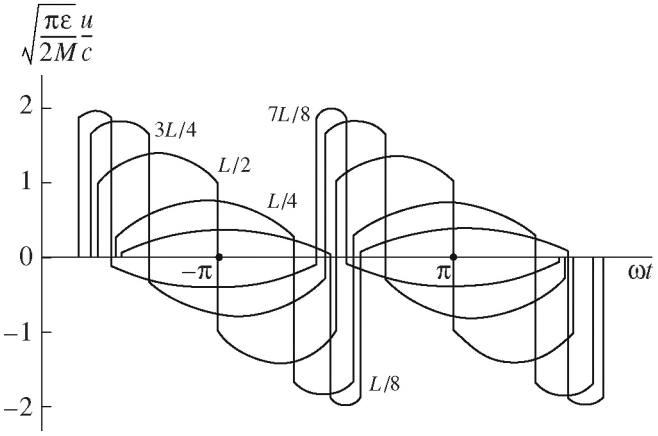

Fig. 3. Established profile of standing waves at $q \longrightarrow \infty$, constructed in various sections of the resonator: $x = L/8$, $L/4$, $L/2$, $3L/4$, $7L/8$.

With large values of the parameter $q \gg 1$, the solution (42) takes the form [19]

$$U = \sqrt{\frac{2M}{\pi\varepsilon}}\left[\cos\frac{\xi}{2} - \frac{3\exp(-2\sqrt{q}\xi)}{1 + 2\exp(-2\sqrt{q}\xi)}\right], \quad 0 \le \xi \le \pi, \quad (43)$$

and at $q \longrightarrow \infty$, it does not depend on linear absorption (i.e., on q) at all:

$$U = \sqrt{\frac{2M}{\pi\varepsilon}}\cos\frac{\xi}{2}\operatorname{sgn}\xi, \quad -\pi \le \xi \le \pi. \quad (44)$$

Figures 2a and 2b show the process of the profiles of a standing wave being established under harmonic boundary oscillations in the middle section of the resonator ($x = L/2$; Fig. 2a) and close to the right face ($x = 7L/8$; Fig. 2b). The profiles have been constructed [21] according to formulas (40), (30) taking into account transformation (36) for the values of "slow time" of $DT = 0.15, 0.3, 0.5, 0.9$. It was supposed that the parameter was equal to $q = 20$.

In contrast to the curves in Fig. 1, the curves in Fig. 2 are smoothed because formation of the shock front for the considered moments of time in traveling waves U have still not terminated. Even at $DT \longrightarrow \infty$, the shock front for the parameter $q = 20$ possesses significant width. A discontinuity occurs at $q \longrightarrow \infty$.

The established profiles of standing waves are shown in Fig. 3 for very strong boundary oscillations, corresponding to $q \longrightarrow \infty$ [21]. The standing wave in Fig. 3 has a form similar to the wave during saw-tooth

boundary oscillations (see Fig. 1). However, the upper areas of impulses of positive and negative polarity are not flat; they have the shape of arcs described by trigonometric functions.

For the wave in Fig. 1, the peak value u/c tends (at $T \longrightarrow \infty$) to a value of $\sqrt{2M/\varepsilon}$, whereas for the wave in Fig. 3, the corresponding value is $2\sqrt{2M/\pi\varepsilon}$.

We proceed now to calculating the energy characteristics of the resonator under harmonic excitation. Note that the steady-state solution (42) satisfies the ordinary differential equation

$$D\frac{d^2U}{d\xi^2} + \pi\varepsilon U\frac{dU}{d\xi} = \frac{M}{2}\sin\xi, \qquad (45)$$

which follows from (26) at $T \longrightarrow \infty$, $\Delta = 0$, and $f(\xi) = -\sin(\xi)$. Integrating (45), we obtain

$$D\frac{dU}{d\xi} + \frac{\pi\varepsilon}{2}(U^2 - C^2) = -\frac{M}{2}\cos\xi. \qquad (46)$$

Since the average over a period should equal zero, $\overline{U} = 0$, from Eq. (46) it follows that the constant is

$$C^2 = \overline{U^2} = \frac{1}{2\pi}\int_0^{2\pi} U^2(\xi)d\xi. \qquad (47)$$

Thus, constant (47) is proportional to the acoustic energy density. Using transformation (36), we can bind nonlinear equation (46) with the linear equation for Mathieu functions:

$$\frac{d^2W}{dz^2} + \left[-\left(\frac{\pi\varepsilon}{D}\right)^2 C^2 + \frac{\pi\varepsilon M}{D^2}\cos 2z\right] = 0, \qquad (48)$$

where $z = \xi/2$. Comparing Eqs. (48) and (39), we arrive at the conclusion that the energy is proportional to the eigenvalue λ_0 of the Mathieu function ce_0 [18]:

$$\overline{U^2} = -\left(\frac{D}{\pi\varepsilon}\right)^2 \lambda_0\left(q = \frac{\pi\varepsilon M}{2D^2}\right). \qquad (49)$$

The full energy stored in the resonator is $E = \rho c^2 V 2\overline{U^2}$.

When there is a weak excitation of $\lambda_0 \approx -q^2/2$ [20], we obtain the known result of linear theory

$$E \approx (M/2D)^2 \rho c^2 V. \qquad (50)$$

For strong boundary oscillations, using a different asymptotic λ_0 at $q \gg 1$ [20], we obtain

$$E = \left[\frac{2M}{\pi\varepsilon} - \frac{2D}{(\pi\varepsilon)^2}\sqrt{2\pi\varepsilon M} + \frac{1}{2}\frac{D^2}{(\pi\varepsilon)^2} + \ldots\right]\rho c^2 V. \qquad (51)$$

At $q \longrightarrow \infty$, coefficient $2/\pi$ in the first (the main) term in parentheses in formula (51) differs from the result of (32), where at $T \longrightarrow \infty$ the corresponding coefficient is 1/3.

Thus, comparison of the results of [21] for saw-tooth and harmonic laws of boundary oscillations of a resonator demonstrates their quality correspondence.

FREQUENCY RESPONSES OF A QUADRATIC-NONLINEAR RESONATOR

The results of the previous section have been obtained for zero detuning. We examine the case of exact correspondence of frequency oscillations of a wall and the frequency of the main mode of the resonator. Taking into account the dependence of the intensity of oscillations on detuning makes it possible to describe the frequency response [22] and by the same token to study the features of the phenomenon of resonance in a nonlinear regime.

The establishment of steady-state oscillations in a resonator occurs as a result of competition between the energy flow from the oscillating wall and losses to linear and nonlinear absorption. The steady state achieved at $T \longrightarrow \infty$ is described by the ordinary differential equations obtained by integration of Eq. (26). If the boundary performs periodic saw-tooth movements of type (27) and if the right-hand side of (26) is described by the expression $-(M/2)\xi/\pi$, the corresponding steady-state equation has the form

$$D\frac{dU}{d\xi} + \frac{\pi\varepsilon}{2}(U^2 - C^2) - \Delta U = \frac{\pi M}{4}\left(\frac{\xi^2}{\pi^2} - \frac{1}{3}\right). \qquad (52)$$

Constant C in (52) has an important physical meaning. As follows from Eq. (26), it is described by formula (47) and is equal to the normalized average intensity of one of the two opposing waves. As well, it is believed that the average over the period from function U is equal to zero, $\overline{U} = 0$.

For a very weak manifestation of linear dissipation, $D \longrightarrow 0$, the solution to Eq. (52) has the form

$$U = \frac{\Delta}{\pi\varepsilon} \pm \sqrt{\left(\frac{\Delta}{\pi\varepsilon}\right)^2 + C^2 + \frac{M}{2\varepsilon}\left(\frac{\xi^2}{\pi^2} - \frac{1}{3}\right)}. \qquad (53)$$

In the case of small Mach numbers, $M \ll 3\Delta^2/\pi^2\varepsilon$, a linear solution is obtained from one of the branches of Eq. (53), namely, from the branch with the minus sign for positive detunings Δ and the branch with the plus sign for negative detunings $\Delta < 0$:

$$U = -\frac{\pi M}{4|\Delta|}\operatorname{sgn}\Delta\left(\frac{\xi^2}{\pi^2} - \frac{1}{3}\right),$$
$$C^2 = \overline{U^2} = \frac{\pi^2 M^2}{180\Delta^2} \ll \frac{M}{3\varepsilon}. \qquad (54)$$

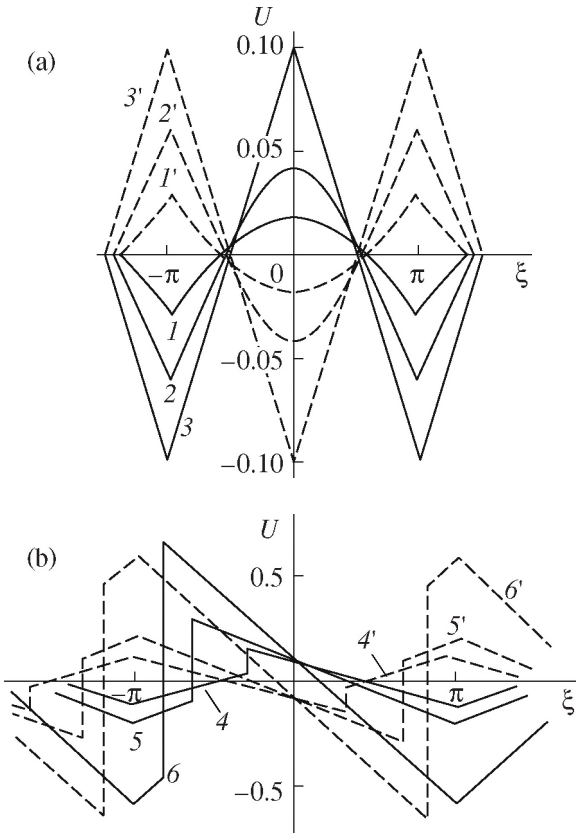

Fig. 4. Time profiles for one of the opposing waves forming the field in the resonator. Wall oscillations are sawtooth in form. Profiles (a) do not contain discontinuities; for curves *1–3*, the value of parameter $10^2(M/2\varepsilon) = 1, 2.25, 4$. Profiles *4–6* contain discontinuities (b); they are constructed for values of $10^2(M/2\varepsilon) = 4, 9, 49$.

The inequality in the latter formula (54) is based on neglect of the term C^2 in deducing the first of formulas (54) from the solution (53).

With an increase in the Mach number right up to the maximum value of M_*, which will be determined later, the wave undergoes progressive nonlinear distortion (Fig. 4a), but it is described as earlier by one of the branches of the solution to (53). Solid lines in Fig. 4a represent positive detunings of $10^2(M/2\varepsilon) = 1, 2.25, 4$. In constructing the profiles, constant C^2 was determined with the solution to an algebraic problem on the eigenvalues:

$$\frac{2\Delta}{\pi\varepsilon} = \sqrt{\left(\frac{\Delta}{\pi\varepsilon}\right)^2 + C^2 + \frac{M}{3\varepsilon}} + \frac{\left(\frac{\Delta}{\pi\varepsilon}\right)^2 + C^2 - \frac{M}{6\varepsilon}}{\sqrt{\frac{M}{2\varepsilon}}} \operatorname{arcsinh} \frac{\sqrt{\frac{M}{2\varepsilon}}}{\left(\frac{\Delta}{\pi\varepsilon}\right)^2 + C^2 - \frac{M}{6\varepsilon}}. \quad (55)$$

The maximal value $M = M_*$, where Eq. (55) has a real solution of $C = \Delta/(\pi\varepsilon\sqrt{3})$, is determined by the condition

$$\sqrt{\frac{M}{2\varepsilon}} = \frac{2|\Delta|}{\pi\varepsilon}, \quad M = \frac{8\Delta^2}{\pi^2\varepsilon} \equiv M_*. \quad (56)$$

At $M = M_*$, a bifurcation occurs and the steady-state form of the wave becomes discontinuous. The shock front appears during every period of the wave, connecting the two branches of the solution to (53).

Let solution U at the moment of fast time ξ_0 be described by the (–) branch of the solution to (53). With an increase in time $\xi > \xi_0$, the solution should perform a jump to the (+) branch; in the opposite case, condition $\bar{U} = 0$ cannot be fulfilled. The moment of the jump $\xi = \xi_{SH}$ corresponds to the situation of compression of the shock front in the wave profile. However, jumps in negative pressure cannot exist in quadratic-nonlinear media in which the speed of propagation increases with an increase in the magnitude of perturbation. Therefore, both branches of the solution to (53) should have one common point in each period. If and only if a common point exists, a transition can occur in it the opposite direction, from the (+) branch to the (–) branch, but without the forbidden jump.

A common point exists if the radicand in the solution to (53) goes to zero, or

$$C^2 = \frac{M}{6\varepsilon} - \left(\frac{\Delta}{\pi\varepsilon}\right)^2. \quad (57)$$

For the now known eigenvalue (57), solution (53) has been simplified:

$$U = \frac{\Delta}{\pi\varepsilon} \pm \sqrt{\frac{M}{2\varepsilon}}\left|\frac{\xi}{\pi}\right|. \quad (58)$$

To discover the state of the front in the wave profile, we apply condition $\bar{U} = 0$ to the solution of (58). This gives

$$\xi_{SH} = -\pi\sqrt{1 - \frac{2\Delta}{\pi}\sqrt{\frac{2}{\varepsilon M}}}. \quad (59)$$

Expression (59) is valid at $M \geq M_*$, (see (56)).

The shape of the discontinuous wave described by the solution of (58), (59) is drawn in Fig. 4b, a continuation of Fig. 4a for the case of Mach numbers of $M \geq M_*$. With increasing M, the discontinuity that has appeared at point $\xi = 0$ in the profile moves toward the state $\xi = -\pi$ (for positive detunings), but it reaches this state only at $M \longrightarrow \infty$ (see Eq. (59)). Solid curves *4–6* in Fig. 4b are constructed for values of $10^2(M/2\varepsilon) = 4, 9, 49$. Dashed curves show a similar behavior of a wave profile for an equivalent negative detuning of $\Delta = -0.1\pi\varepsilon$. In this case, the rupture at $M = M_*$, appears at

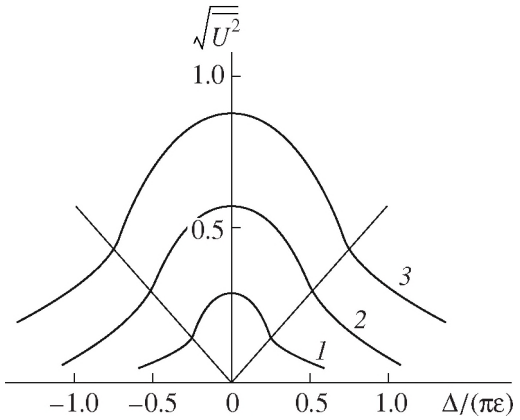

Fig. 5. Nonlinear frequency response determined as the dependence of the mean-square velocity as a function of frequency. Curves *1–3* are constructed for values of $(M/2\varepsilon) = 0.25, 1.00, 2.25$. The periodic boundary oscillations are saw-tooth in form.

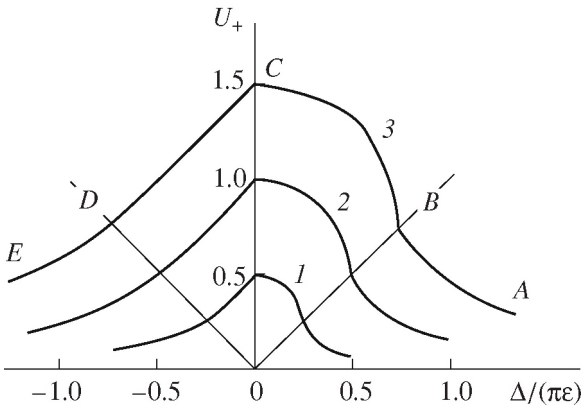

Fig. 6. Nonlinear frequency response determined as the dependence of the positive peak value as a function of frequency. Curves *1–3* are constructed for values of $(M/2\varepsilon) = 0.25, 1.00, 2.25$. The periodic boundary oscillations are saw-tooth in form.

point $\xi = 0$, but moves toward the state $\xi = +\pi$ at $M \longrightarrow \infty$.

In Fig. 5, the nonlinear frequency characteristic is shown. Curves *1–3* constructed for various Mach numbers of $(M/2\varepsilon) = 0.25, 1.00, 2.25$ give the dependence $C = \sqrt{U^2}$ from detuning (18). Straight lines $\sqrt{U^2} = \Delta/(\pi\varepsilon\sqrt{3})$ are separatrices. Below these lines, the curves in Fig. 5 have been constructed to with the help of the solutions to (53), (55) for wave profiles not containing discontinuities. Precisely on the lines, the Mach number $M = M_*$. Above the straight lines, the response has been constructed on the basis of the discontinuity solution to (58), (59).

The dependence of the mean-square speed $C = \sqrt{U^2}$ on detuning, depicted in Fig. 5, is not the only possible determination of the frequency response of a nonlinear resonator. Sometimes it is important to know the dependence $U_+(\Delta)$, where U_+ is the positive peak value of oscillation speed U. The response determined in this way is depicted in Fig. 6 by the solid curves for three values of $(M/2\varepsilon) = 0.25, 1.00, 2.25$. An analytical representation of sectors *AB*, *BC*, *CD*, and *DE* is given, respectively, by the formulas

$$\frac{\Delta}{\pi\varepsilon} - \sqrt{\left(\frac{\Delta}{\pi\varepsilon}\right)^2 + C^2 - \frac{M}{6\varepsilon}},$$

$$\frac{\Delta}{\pi\varepsilon} + \sqrt{\frac{M}{2\varepsilon} - 2\frac{\Delta}{\pi\varepsilon}\sqrt{\frac{M}{2\varepsilon}}}, \quad -\frac{|\Delta|}{\pi\varepsilon} + \sqrt{\frac{M}{2\varepsilon}},$$

$$-\frac{|\Delta|}{\pi\varepsilon} + \sqrt{\left(\frac{\Delta}{\pi\varepsilon}\right)^2 + C^2 + \frac{M}{3\varepsilon}}.$$

Here the eigenvalue C^2 is determined by Eq. (55).

Another important case corresponds to the harmonic law of boundary vibration. As well, the ordinary differential equation (52) has the form

$$D\frac{dU}{d\xi} + \frac{\pi\varepsilon}{2}(U^2 - C^2) - \Delta U = \frac{M}{2}\cos\xi. \qquad (60)$$

If the linear dissipation is weak, $D \longrightarrow 0$, the solution is given by the formula

$$U = \frac{\Delta}{\pi\varepsilon} \pm \sqrt{\left(\frac{\Delta}{\pi\varepsilon}\right)^2 + C^2 + \frac{M}{\pi\varepsilon}\cos\xi}, \qquad (61)$$

which is analogous to solution (53) for a saw-tooth form of boundary oscillation. For small Mach numbers, $M \ll \Delta^2/\pi\varepsilon$, we obtain the linear solution

$$U = -\frac{M}{2|\Delta|}\operatorname{sgn}\Delta\cos\xi, \quad C^2 = \overline{U^2} = \frac{M^2}{8\Delta^2} \ll \frac{M}{\pi\varepsilon}. \qquad (62)$$

With increasing M, the form of the wave is distorted (Fig. 7a), but it is still nonetheless described by one branch of the solution to (61). Solid curves *1–3* in Fig. 7a have been constructed for positive detuning of $\Delta = 0.1\pi\varepsilon$, and the dashed curves, for the same values but for a negative detuning. The increase in the number of the curve corresponds to any increase in amplitude of boundary oscillations: $10^3(M/2\varepsilon) = 5.6, 9.1, 12.3$. In constructing curves, constant C^2 was found from the solution to an algebraic problem for the eigenvalues (see (55)):

$$\frac{\Delta}{\pi\varepsilon} = \frac{2}{\pi}\sqrt{\left(\frac{\Delta}{\pi\varepsilon}\right)^2 + C^2 + \frac{M}{\pi\varepsilon}} \times E\left[\frac{\frac{2M}{\pi\varepsilon}}{\sqrt{\left(\frac{\Delta}{\pi\varepsilon}\right)^2 + C^2 + \frac{M}{\pi\varepsilon}}}\right]. \qquad (63)$$

Here, E is a full elliptic integral of the second kind [23].

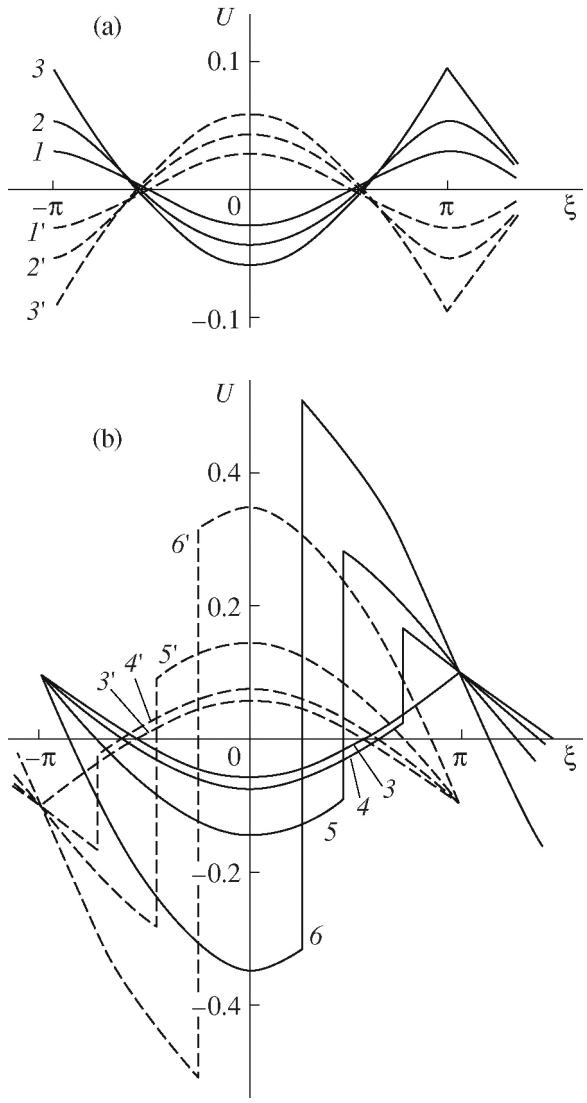

Fig. 7. (a) Time profile of one of two opposing waves that do not contain discontinuities for a value of parameter $10^3(M/2\varepsilon) = 5.6, 9.1, 12.3$ (curves *1–3*). (b) Discontinuous profiles for values of $10^2(M/2\varepsilon) = 1.5, 3, 10$ (curves *4–6*).

It is convenient to seek the solution, having written (63) in parametric form (m is the parameter):

$$C^2 = \frac{M}{\pi\varepsilon}\left[\frac{2}{m} - 1 - \frac{8}{\pi^2}\frac{E^2(m)}{m}\right],$$
$$\frac{\Delta}{\pi\varepsilon} = \pm\frac{2\sqrt{2}}{\pi}\sqrt{\frac{M}{\pi\varepsilon}}\frac{E(m)}{\sqrt{m}}. \quad (64)$$

The argument of function $E(m)$ is determined in the area of $0 \le m \le 1$ [23]. From (63), it follows that the corresponding area of the change in detuning is given by the inequalities

$$\frac{2\sqrt{2}}{\pi}\sqrt{\frac{M}{\pi\varepsilon}} \ll \frac{|\Delta|}{\pi\varepsilon} < \infty \Rightarrow M \ll \frac{8}{\pi\varepsilon}\Delta^2 \equiv M_*. \quad (65)$$

At $M = M_*$, a bifurcation takes place and the standing wave becomes discontinuous. A jump appears in each period of the profile, combining the two branches of the solution (61). For a discontinuous wave,

$$C^2 = \frac{M}{\pi\varepsilon} - \left(\frac{\Delta}{\pi\varepsilon}\right)^2. \quad (66)$$

For eigenvalue (66), the solution (61) the takes the form

$$U = \frac{\Delta}{\pi\varepsilon} \pm \sqrt{\frac{2M}{\pi\varepsilon}}\left|\cos\frac{\xi}{2}\right|. \quad (67)$$

The location of the front is found from the condition $\overline{U} = 0$ and is determined by the equation

$$\sin\frac{\xi_{SH}}{2} = \frac{\Delta}{2}\sqrt{\frac{\pi}{2\varepsilon M}}. \quad (68)$$

From the latter expression (68), it follows that condition $|\sin(\xi_{SH}/2)| \le 1$ is equivalent to the condition $M \ge M_*$ (65).

The solution to (67), (68) is depicted in Fig. 7b, which is a continuation of Fig. 7a for the case of large Mach numbers. Curve *3* in Fig. 7b, corresponding to $M = M_*$, coincides with curve *3* in Fig. 7a. As the Mach number increases in the area of $M \ge M_*$, the discontinuity that appeared first at point $\xi = \pi$ of the profile (for $\Delta > 0$), tends toward the state $\xi = 0$, which is achieved at $M \longrightarrow \infty$ (see (68)). Solid curves *4–6* in Fig. 7b have been constructed for values of $10^2(M/2\varepsilon) = 1.5, 3, 10$. Dashed curves in Fig. 7b demonstrate an analogous behavior for the profile with equivalent values for the negative detuning $\Delta = -0.1\pi\varepsilon$. In this case, a discontinuity arises at $M = M_*$ at point $\xi = -\pi$ and it shifts with increasing Mach number to the state $\xi = 0$.

Figure 8 depicts the nonlinear frequency characteristic for the case of harmonic wall oscillations of the resonator. Curves *1–5* have been constructed for various Mach numbers $10^2(M/2\varepsilon) = 1, 4, 9, 16, 25$. They demonstrate the dependence of the mean-square velocity $C = \sqrt{\overline{U^2}}$ on detuning. The straight lines

$$\sqrt{\overline{U^2}} = \pm\frac{\Delta}{\pi\varepsilon}\sqrt{\frac{\pi^2}{8} - 1} \quad (69)$$

are separatrices. Beneath these lines, the curves of Fig. 8 have been constructed with the help of the solution (62) for profiles not containing discontinuities. $M = M_*$ if points fall on the straight lines described by (69). Above the lines of (69), another solution (67), (68) is used to find the nonlinear frequency response of the system.

Here and earlier, the Q-factor can be determined in two ways: as the ratio of the amplitude of field oscilla-

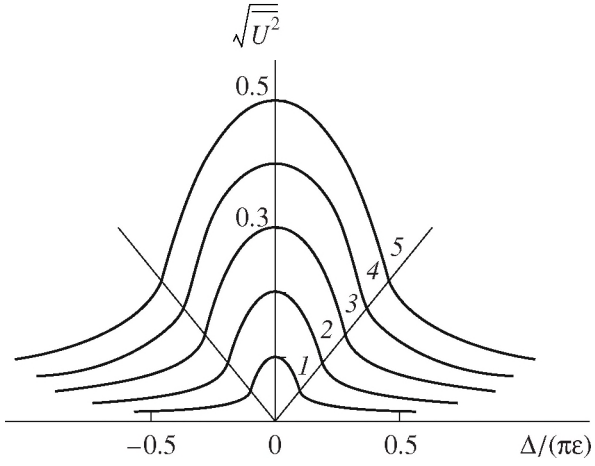

Fig. 8. Nonlinear frequency response determined as the dependence of the mean-square vibration velocity in the resonator as a function of frequency for the harmonic law of boundary movement. Curves *1–5* correspond to various values of parameter $10^2(M/2\varepsilon) = 1, 4, 9, 16, 25$.

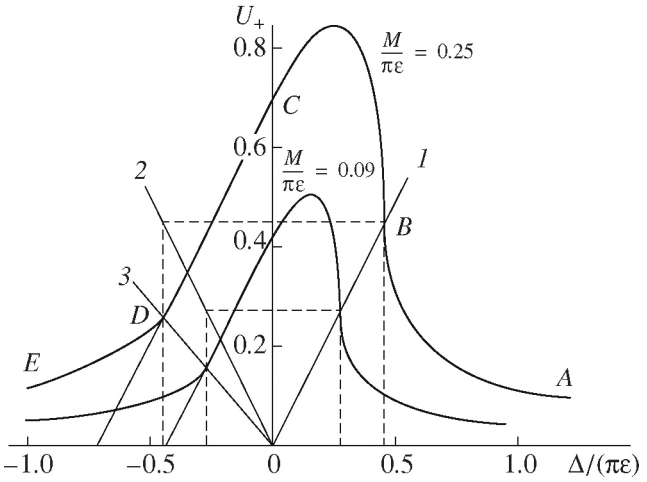

Fig. 9. Nonlinear frequency response determined as the dependence of the positive peak of the vibration velocity in the resonator as a function of frequency for the harmonic law of boundary movement. The amplitude of boundary oscillations is supposed equal to $(M/2\varepsilon) = 0.09, 0.25$.

tions in the resonator to the amplitude of wall oscillations (at $\Delta = 0$) and as the ratio of the resonance frequency to the characteristic width of the frequency response. The first definition leads to the formula (see (34))

$$Q_{NL} = \frac{c}{A}\sqrt{\overline{U^2}}\bigg|_{\Delta=0} = \frac{c}{A}\sqrt{\frac{M}{\pi\varepsilon}} = \frac{1}{\sqrt{\pi\varepsilon M}}. \qquad (70)$$

The second definition gives an expression that differs only in the numerical coefficient:

$$Q_{NL} = \frac{1}{\Delta} = \frac{\pi}{2\sqrt{2}}\frac{1}{\sqrt{\pi\varepsilon M}}. \qquad (71)$$

Dependence $U_+(\Delta)$, where U_+ is the peak positive value of oscillation rate U, is depicted by the solid curves in Fig. 9 for two values of $(M/2\varepsilon) = 0.09, 0.25$. The analytical description of sectors AB, BC, CD, and DE is given by the formulas

$$\frac{\Delta}{\pi\varepsilon} - \sqrt{\left(\frac{\Delta}{\pi\varepsilon}\right)^2 + C^2} - \frac{M}{\pi\varepsilon},$$

$$\frac{\Delta}{\pi\varepsilon} + \sqrt{2}\sqrt{\frac{M}{\pi\varepsilon} - \frac{\pi^2}{8}\left(\frac{\Delta}{\pi\varepsilon}\right)^2}, \quad -\frac{|\Delta|}{\pi\varepsilon} + \sqrt{2}\sqrt{\frac{M}{\pi\varepsilon}},$$

$$-\frac{|\Delta|}{\pi\varepsilon} + \sqrt{\left(\frac{\Delta}{\pi\varepsilon}\right)^2 + C^2} + \frac{M}{\pi\varepsilon}.$$

Here the eigenvalue C^2 is determined by Eq. (64). Straight lines *1* and *2* here are the same separatrices in Fig. 8. Line *3*, which divides sectors CD and DE, is given by the formula

$$U_+ = \left(\frac{\pi}{2} - 1\right)\frac{\Delta}{\pi\varepsilon}. \qquad (72)$$

Note that the peak positive value U_+ reaches the crest of the shock front only for sector BC. For the other three sectors of the frequency characteristic, U_+ lies in the smooth sector of the wave profile. In contrast to the curves of Fig. 8, the maximum value of U_+ in Fig. 9 corresponds not to $\Delta = 0$, but to a certain positive detuning:

$$(U_+)_{\max} = \sqrt{2}\left(1 + \frac{4}{\pi^2}\right)\sqrt{\frac{M}{\pi\varepsilon}},$$
$$\left(\frac{\Delta}{\pi\varepsilon}\right)_{\max} = \frac{2\sqrt{2}}{\pi\sqrt{1 + \pi^2/4}}\sqrt{\frac{M}{\pi\varepsilon}}. \qquad (73)$$

In conclusion, we have the approximate formulas for the mean intensity of the field in a resonator in the case of weak and strong manifestation of nonlinearity taking into account linear dissipation:

$$\overline{U^2} = \frac{M^2}{8D^2} - \frac{7}{2048}\frac{(\pi\varepsilon)^2 M^4}{D^6},$$
$$\overline{U^2} = \frac{M}{\pi\varepsilon} - \sqrt{2}\frac{D}{\pi\varepsilon}\sqrt{\frac{M}{\pi\varepsilon}} + \frac{1}{4}\left(\frac{D}{\pi\varepsilon}\right)^2 + \frac{1}{16}\left(\frac{D}{\pi\varepsilon}\right)^4\frac{\pi\varepsilon}{M}. \qquad (74)$$

It is possible to simultaneously take into account detuning and dissipation in the case when nonlinear

effects are weakly manifested:

$$\overline{U^2} = \frac{M^2}{8(\Delta^2 + D^2)} - \frac{(\pi\varepsilon)^2 M^4}{512} \frac{7D^2 - 5\Delta^2}{(\Delta^2 + D^2)^3 (\Delta^2 + 4D^2)}. \quad (75)$$

To deduce formula (75), it is necessary to solve Eq. (60) by the perturbation method and to calculate the first four approximations. Formula (75) passes to the first of formulas (74) at zero detuning.

When nonlinearity is strongly manifested, it is possible to simultaneously take into account dissipation, taking into consideration the wave profile by means of matched asymptotic expansions method [22, 26]. The result of averaging is as follows:

$$\overline{U^2} = \left[\frac{M}{\pi\varepsilon} - \left(\frac{\Delta}{\pi\varepsilon}\right)^2\right] - \sqrt{2}\frac{D}{\pi\varepsilon}\sqrt{\frac{M}{\pi\varepsilon} - \frac{\pi^2}{8}\left(\frac{\Delta}{\pi\varepsilon}\right)^2}. \quad (76)$$

When there is exact resonance, from (76) we obtain the first two terms of the second formula of (74), which follows from the theory of Mathieu functions.

Note that the wave profiles for the case of periodic boundary oscillations were constructed in [24], but the frequency response (see the curves in Figs. 8, 9) was calculated later [22].

AN INCREASE IN Q-FACTOR AS LOSSES ARE INTRODUCTED INTO THE RESONATOR

There exists a paradoxical, at first glance, phenomenon: an outflow of energy from the cavity of the resonator, performed in the appropriate manner, leads not to a weakening of nonlinear oscillations, but, on the contrary, to a noticeable strengthening. The effect of an increase in the Q-factor and the energy accumulating in it is well expressed in such cases when the frequencies of the high harmonics generated in a nonlinear medium are close to the eigenfrequencies of the resonator. An acoustic resonator with selective losses is an important example of a system possessing the necessary properties.

The spectrum of eigenfrequencies of a resonator with rigid walls is equidistant, $\omega_n = n\omega_0 = n\pi c/L$. Therefore, a generated harmonic with number n is the nth mode, and in the resonator, a cascade of nonlinear processes takes place that lead to an effective upward jump in energy across the spectrum. In the high-frequency area, the energy of oscillations is intensively absorbed as a result of dissipative processes usually connected to the viscosity and thermal conductivity of the medium.

The general ideas on controlling wave interactions at the expense of introducing selective losses have been set down in [9,10]. In the given case, it is necessary to introduce an absorber at frequency $2\omega_0$; quenching of the second harmonic disrupts the cascade process of transfer of energy upward across the spectrum or, in other words, it quenches the formation of shock fronts. Technically, losses at frequency $2\omega_0$ can be brought about either by the introduction of resonance scatterers in the bulk of the medium (for instance, gas bubbles in a liquid) or by using selective boundaries (for instance, borders that are transparent to a wave at $2\omega_0$ and that reflect all other frequencies inward [11]).

We represent a field oscillating between the walls of a resonator $x = 0$ and $x = L$ as the superposition of two opposing nonlinear waves (see the section method for calculating the characteristics of nonlinear resonators). The auxiliary function u describing the "right" wave of the vibration velocity obeys the equation

$$\frac{1}{c}\frac{\partial u}{\partial t} - \frac{\varepsilon}{c^2}u\frac{\partial u}{\partial \tau} - \frac{b}{2c^3}\frac{\partial^2 u}{\rho \partial \tau^2} = \frac{A}{2L}\sin\omega t - \frac{\alpha}{c}b_2(t)\sin 2\omega t. \quad (77)$$

Here, t is slow time, describing the establishment processes in the resonator; τ is fast time, describing oscillations; α is the coefficient of selective absorption; and $b_2(t)$ is the amplitude of the second harmonic:

$$b_2(t) = \frac{2}{\pi}\int_0^\pi u(t, \tau)\sin 2\omega\tau d(\omega\tau), \quad (78)$$

which is a priori unknown. Thus, model (77), (78) is an integrodifferential equation. In cases when the right-hand side of (77) is known, model (77) passes to an inhomogeneous equation of the Burgers type [18].

For convenience we use the dimensionless variables

$$V = \frac{u}{u_0}, \quad \theta = \omega\tau, \quad T = \frac{1}{t_{SH}}; \quad t_{SH} = \frac{c}{\varepsilon\omega u_0}, \quad u_0 = \sqrt{\frac{Ac}{2\pi\varepsilon}}. \quad (79)$$

Here, t_{SH} is the characteristic nonlinear time in which a discontinuity is able to form in the wave and u_0 is the characteristic amplitude. Equations (77), (78), taking into account (79), take the form

$$\frac{\partial V}{\partial T} - V\frac{\partial V}{\partial \theta} - \Gamma\frac{\partial^2 V}{\partial \theta^2} = \sin\theta - D\sin 2\theta\frac{2}{\pi}\int_0^\pi V(T, \theta')\sin 2\theta' d\theta'. \quad (80)$$

Here the dimensionless numbers

$$\Gamma = \frac{b\omega}{2\varepsilon\rho c u_0} = \frac{t_{SH}}{t_{DIS}}, \quad D = \frac{\alpha c}{\varepsilon\omega u_0} = \alpha t_{SH} \quad (81)$$

are determined by the ratio of nonlinear time t_{SH} to the time of regular dissipative (viscous) absorption (num-

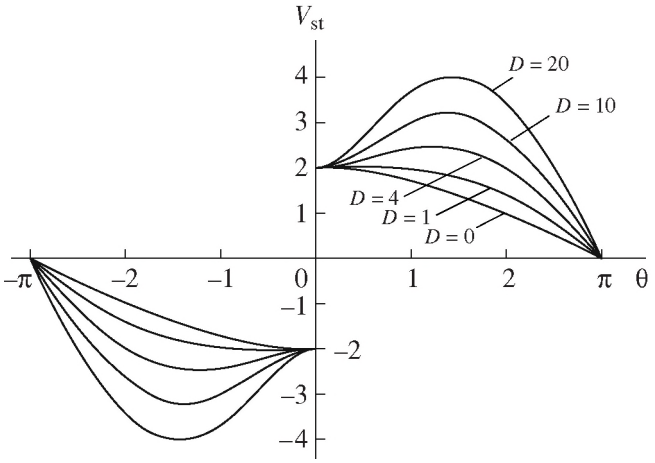

Fig. 10. Profiles of one period of one of the two traveling waves forming the nonlinear field in the resonator with selective losses at a frequency of the second harmonic of $D = 0, 1, 4, 10, 20$.

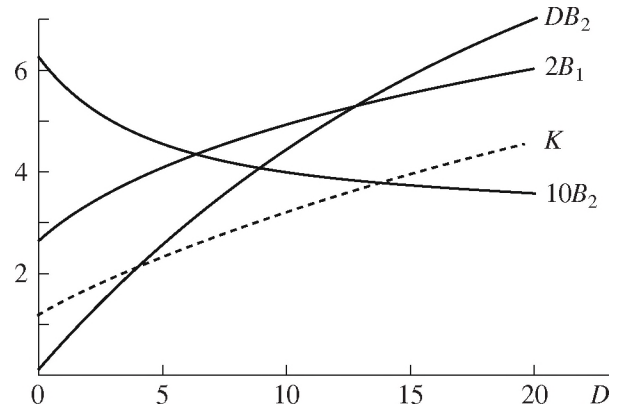

Fig. 11. Dependences of the amplitudes of the first and second harmonics, as well as of the product of DB_2, for various values of selective absorption D (solid lines) and strengthening coefficient of oscillation energy K accumulated in the cavity of the resonator.

ber Γ), or to the characteristic time α^{-1} of selective absorption (number D).

To calculate the process of excitation of induced oscillations in the resonator, it is necessary to solve (80) with the zero initial condition $V(T = 0, \theta) = 0$. At large values of slow time, $T \longrightarrow \infty$, balance is achieved between the arrival of the energy from the source (an oscillating wall) and losses of three types: viscous, nonlinear, and selective. Analysis of the established oscillations can be performed analytically. As well, in the steady state, nonlinearity is expressed more strongly than anything; therefore this regime is of the most interest. The solution has the form [25]

$$\frac{V_{ST}(\theta)}{\sqrt{2}} = \pm\left[(1+\cos\theta) + D(1-\cos^2\theta)\frac{2}{\pi}\int_0^{\pi} V_{ST}(\theta')\sin 2\theta' d\theta'\right]^{1/2}. \quad (82)$$

A plus sign is taken for the half-period $0 < \theta \le \pi$; a minus sign, for $-\pi \le \theta < 0$. In the neighborhood of $\theta = 0$, a shock front forms. Having no interest in its structure, we have placed the parameter $\Gamma = 0$ into the solution (82). Allowance for the finiteness of Γ can be done by the method of matched asymptotic expansions method (see, e.g., [26]) and it can give only small corrections (in the regime of strongly expressed nonlinearity) to the energy characteristics of the field.

The profiles of one period of oscillations (82) are depicted in Fig. 10 for various values of selective absorption $D = 0, 1, 4, 10, 20$. The profile in the presence of only nonlinear absorption ($D = 0$) corresponds to the known solution of the inhomogeneous Burgers equation [19]

$$V_{ST}(\theta) = 2\cos(\theta/2)\,\mathrm{sgn}\,\theta. \quad (83)$$

With any increase in selective absorption D, the dimensionless amplitude of discontinuity in Fig. 10 does not increase. However, an increase in perturbation V_{ST} is observed in the smooth sectors of the profile. At $D \gg 1$, oscillation occurs nearly according to the harmonic law $V_{ST} \approx V_0 \sin\theta$ and only at point $\theta = 0$ is a jump at the small relative value of $2 \ll V_0$ preserved.

Thus, with an increase in D, a significant drop in amplitude B_2 of the second harmonic 2ω is observed. The beginning of this process is shown in Fig. 11. Quenching of wave 2ω slows the energy changeover to higher harmonics 3ω, 4ω,.... Therefore, energy accumulates in the wave of the main frequency ω, which practically does not attenuate at all. The increase in the amplitude of the first harmonic $B_1(D)$ is also shown in Fig. 11. Here as well, the dependence $DB_2(D)$ is given. The maximal perturbation value (82) $V_{ST} = 2$ is achieved at $\theta = 0$ for $DB_2 \le 0.5$, but for $DB_2 > 0.5$, the maximum (see Fig. 10) shifts to point θ_{max}, where

$$V_{max}(\theta_{max}) = \frac{1+2DB_2}{\sqrt{2DB_2}}, \quad \theta_{max} = \arccos\frac{1}{2DB_2}. \quad (84)$$

The mean intensity

$$I = \overline{V_{ST}^2} = 2 + DB_2(D) \quad (85)$$

also increases with strengthening of selective absorption.

The Q-factor of the resonator in the regime of nonlinear oscillations, which have a complex spectrum, can be determined as the ratio of the maximal velocity in a

standing wave $2u_{\max}$ to the amplitude of the velocity of boundary oscillations:

$$Q = \frac{2u_{\max}}{A} = \sqrt{\frac{2c}{\pi\varepsilon A}}\Phi(2DB_2);$$
$$\Phi(x \equiv 2DB_2) = \frac{1+x}{\sqrt{x}}, \quad x > 1; \tag{86}$$
$$\Phi = 2, \quad x \le 1.$$

It is also possible to determine the square of the Q-factor by means of the ratio of the mean intensities of these oscillations.

$$Q^2 = \frac{2\overline{u^2}}{A^2/2} = \frac{2c}{\pi\varepsilon A}(2 + DB_2). \tag{87}$$

Both formulas (86), (87) describe the increase in Q-factor with an increase in selective absorption D.

Estimates according to these formulas show that, if the right wall $x = L$ of the resonator selectively lets out 98% of the power of decreasing radiation at the frequency of the second harmonic, the Q-factor of the resonator increases by approximately a factor of 3.5, but the energy of oscillations increase by an order of magnitude [25].

GEOMETRICAL NONLINEARITY CAUSED BY BOUNDARY MOBILITY

As mentioned at the beginning of this paper, there are methods for suppressing linear and nonlinear losses in a resonator. When it is possible to reduce these losses to a minimum, a process having a geometrical nature can become the defining one. This is caused by the nonlinear character of the connection between the law of motion of a radiating surface and the shape of the traveling wave. In problems on radiation of waves, manifestations of such nonlinearity do not accumulate; they are therefore noticeably expressed only at rates of movement comparable to the velocity of sound. Studies [27, 28] describe the processes of distortion of noise spectra created by intensive chaotic oscillations of a piston in a medium with a small velocity of sound (for example, in bubbly fluids), as well as interactions of a regular signal and noise (signal attenuation in the presence of the noise component, an avalanche-type broadening of the noise spectrum due to generation of the signal harmonics, etc.).

At the same time, effects of such geometric (boundary) nonlinearity can be strongly expressed in a resonator where the process of the accumulation of such effects with time is possible. As a result, as shown below, in the steady-state regime, nonlinear effects are determined by the ratio of two small parameters $M = A/c$ and Δ (where A is the amplitude of the velocity for a radiating surface, c is the velocity of sound, and Δ is the detuning from an exact resonance, the minimum values of which are $\Delta \sim Q^{-1}$). The ratio M/Δ can be a relatively large value in hi-Q resonators or during intensive pumping.

We examine a layer of a linear medium between $x = 0$ and $x = L$. The left boundary of the layer completes oscillations and shifts according to the law $x = X(t)$ relative to the mean state $x = 0$. The right boundary $x = L$ is immovable.

We write the solution of one-dimensional equations of linear acoustics for waves with velocity u and pressure p in the form

$$u = F\left(t - \frac{x-L}{c}\right) - F\left(t + \frac{x-L}{c}\right),$$
$$\frac{p}{\rho c} = F\left(t - \frac{x-L}{c}\right) + F\left(t + \frac{x-L}{c}\right). \tag{88}$$

Here c and ρ are the velocity of sound and the density of the medium, and $F(t)$ is the shape of the traveling wave. Record (88) ensures fulfillment of boundary conditions $u(t, x = L) = 0$. The form of the function $F(t)$ for the established process is determined by the second boundary condition: on the shifted left wall of the resonator, the vibration velocity of the medium should coincide with velocity of the moving wall, i.e.,

$$u(t, x = X(T)) = dX/dt. \tag{89}$$

Hence,

$$\frac{dX}{dt} = F\left[t + \frac{L}{c} - \frac{1}{c}X(t)\right] - F\left[t - \frac{L}{c} + \frac{1}{c}X(t)\right]. \tag{90}$$

With the known law of motion $X(t)$, expression (90) is a functional difference equation for determining the wave form $F(t)$. The inverse problem is of interest when it is necessary to determine the law $X(t)$ of boundary motion, resulting in a wave with the given profile $F(t)$ being established in the resonator. Note that the inverse problem has an independent value; since its solution is combined with simpler mathematical procedures, we begin our analysis precisely with the inverse problem.

We examine the important case of harmonic oscillations of a medium, supposing

$$F(t) = -\frac{A}{2}\frac{\cos\omega t}{\sin kL}, \quad k = \frac{\omega}{c}. \tag{91}$$

For this, the solution to (88),

$$u = A\frac{\sin k(L-x)}{\sin kL}\sin\omega t, \tag{92}$$

describes the linear induced oscillations of the layer. If we neglect the movement of the left wall from the mean state $x = 0$, the law of its motion, as is seen from (92), should also be harmonic:

$$X'(t) = u(t, x = 0) = A\sin\omega t. \tag{93}$$

At $kL = \pi n$, $n = 1, 2\ldots$, resonance begins and the amplitude of oscillations (92) increases without limit nearly everywhere, with the exception of point $x = 0$

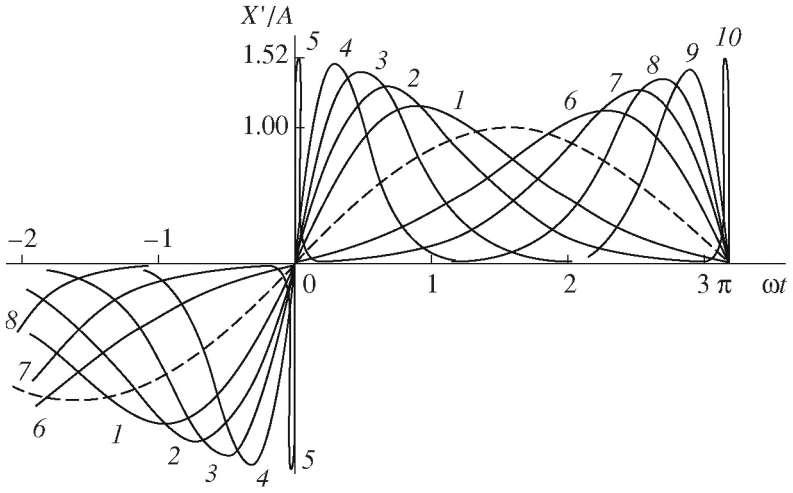

Fig. 12. Form of wall oscillations resulting in effective inflow of energy under conditions where boundary nonlinearity is manifested. For curves *1–4*, the detuning is supposed equal to $M/\Delta = 1, 2, 4, 10$. For curve *5*, the detuning is $M/\Delta \gg 1$. Curves *6–10* are constructed for the same $M/|\Delta|$ as curves *1–5*, but for them, the detuning is negative, $\Delta < 0$.

and the nodes of the standing wave (92). When the established amplitude values are limited by dissipative processes, to find the increase in the level of the limit, it is necessary to increase the amplitude of wall oscillations. Such an increase makes it necessary to take into account movement of the boundary, and the law of its movement (93) changes.

Thus, we pose the following question: how should the left boundary of the resonator oscillate so that, inside the layer, movement of the medium in the form of (92) is preserved? Having determined $X(t)$, we, using this, can demonstrate the method of approximation to resonances under very high excitation.

Expression (90) for the known function $F(t)$ (91) takes the form of an ordinary differential equation:

$$\frac{dX}{dt} = \frac{A}{\sin kL}\sin[kL - kX(t)]\sin\omega t. \qquad (94)$$

Solving (94), we obtain

$$\cos[kX(t) - kL] = \frac{\cos kL - \tanh\beta}{1 - \cos kL\tanh\beta},$$
$$\beta = \frac{A\cos\omega t}{c\sin kL} + D, \qquad (95)$$

where D is the integration constant.

For definiteness, we now look at the neighborhood of the main resonance, setting $kL = \pi + \Delta$. Here, detuning $\Delta = \pi(\omega - \omega_0)/\omega_0$ is taken to be small, which corresponds to the smallness of the relative width of the resonance curve, the central frequency of which is $\omega_0 = \pi c/L$. We will also take as small the displacement of the wall in comparison to the wavelength $k|X| \ll 1$. In other words, the acoustic Mach number $M = A/c$—the ratio of amplitude of the vibration velocity A for particles in the medium to the velocity of sound c—is presumed small.

In solving this, the solution (95) is simplified and leads to the following form:

$$kX(t) = \Delta\left[1 - I_0^{-1}\left(\frac{M}{\Delta}\right)\exp\left(\frac{M}{\Delta}\cos\omega t\right)\right]. \qquad (96)$$

Here, I_0 is the modified Bessel function. In going from (95) to (96), constant D is chosen such that the mean, averaged over period, movement of the wall is equal to zero. The velocity of the boundary is equal to

$$X'(t) = AI_0^{-1}\left(\frac{M}{\Delta}\right)\sin\omega t\exp\left(\frac{M}{\Delta}\cos\omega t\right). \qquad (97)$$

Expansion of function (97) into Fourier series over sine,

$$X'(t) = 2A\left[I_0\left(\frac{M}{\Delta}\right)\frac{M}{\Delta}\right]^{-1}\sum_{n=1}^{\infty} nI_n\left(\frac{M}{\Delta}\right)\sin n\omega t, \qquad (98)$$

determines the spectral component of wall oscillations; the term of series (98) with the number n gives the expression for the amplitude of the nth harmonic. Finally, we give here the formula for the mean intensity of boundary oscillations,

$$\overline{X'^2} = \frac{A^2}{2}I_1\left(2\frac{M}{\Delta}\right)\left[\frac{M}{\Delta}I_0^2\left(\frac{M}{\Delta}\right)\right]^{-1}. \qquad (99)$$

Setting $M \longrightarrow 0$ in expressions (96)–(99), we arrive at the obvious result for the linearized problem:

$$X = -\frac{A}{\omega}\cos\omega t, \quad X' = A\sin\omega t, \quad \overline{X'^2} = \frac{A^2}{2}. \qquad (100)$$

Here it is very important that small parameters M and Δ enter formulas (96)–(99) in the form of ratios. This means that, in the neighborhood of resonance, nonlin-

ear distortions can be noticeably expressed even at small Mach numbers M. This is the difference between problems on induced oscillations of a resonator with movable boundaries of waves radiating from an oscillating piston into an infinite medium. In the latter case, the effects of geometric nonlinearity in passing from $X'(t)$ to $F(t)$ become noticeable only for rates of movement of the piston comparable to the speed of sound [27, 28].

In the opposite case, in a high-Q resonator, small nonlinear distortions in connection with the finiteness of wall movement from the median state $x = 0$ can accumulate with time and lead to strongly expressed nonlinear effects.

Figure 12 shows the solution (97) to inverse problem [29] for the velocity of the left boundary of the resonator. Precisely this movement of the wall leads to establishment of linear, in the form of (92), oscillations of the medium. The dashed curve in Fig. 12 corresponds to small oscillations of wall movement or large detunings from resonance: $M/\Delta \ll 1$. Curves *1–4* correspond to positive detunings and ratios of M/Δ of 1, 2, 4, and 10, respectively. Clearly, with increasing M/Δ, the shapes of the curves are distorted; the spectrum is enriched in harmonics (98). At large values of M/Δ, to maintain harmonic oscillations of the medium, it is necessary to excite the resonator with short bipolar jerkings of the wall (curve *5* in Fig. 12) one after another with a period of $2\pi/\omega$. The form of these jerkings and the maximum value (at $M/\Delta \longrightarrow \infty$) of their amplitude are described by the following expressions:

$$X'(t) = \sqrt{4\pi}A\left(\frac{M}{2\Delta}\omega^2 t^2\right)^{1/2}\exp\left(-\frac{M}{2\Delta}\omega^2 t^2\right),$$
$$X'_{\max} = A\sqrt{\frac{2\pi}{e}} \approx 1.52A. \quad (101)$$

The intensity (99) of boundary oscillations with an increase in M/Δ decreases, and at large values of this parameter, it behaves as

$$\overline{X'^2} = \frac{A^2}{2}\sqrt{\pi\frac{\Delta}{M}} = \frac{\sqrt{\pi}}{2}c^2M^{3/2}\Delta^{1/2}. \quad (102)$$

Curves *6–10* in Fig. 12 have been constructed for the same $M/|\Delta|$ as curves *1–5*, but for these, the value for detuning is negative, $\Delta < 0$.

Note that the energy stored in the resonator of a medium oscillating according to law (92),

$$E = \int_0^L \overline{u^2}\,dx \approx \frac{A^2L}{4\Delta^2} = \frac{Lc^2}{4}M^2\Delta^{-2}, \quad (103)$$

on the contrary, increases with an increase in $M/|\Delta|$. Thus, the ratio of the intensity of oscillations of source $\overline{X'^2}$ to the stored energy E (103)—a constant in the linear case—with allowance for boundary movement decreases as $A^{-1/2}$.

We now pass to solving direct problem [29], taking into consideration that movement of the left boundary of the resonator occurs according to the harmonic law

$$X' = A\sin\omega t, \quad X = -(A/\omega)\cos\omega t. \quad (104)$$

Substituting (104) into boundary condition (90), we arrive at the following form:

$$\sin\omega t = V(\omega t + kL + M\cos\omega t) - V(\omega t - kL - M\cos\omega t). \quad (105)$$

Here, it is designated $V = F/A$, $M = A/c$. It is clear that the unknown function $V(\omega t)$ should be periodic (with a period of 2π) and the even function of its argument.

In the neighborhood of the main resonance $kL = \pi + \Delta$, formula (105) is written as follows:

$$V(y + M\cos y - \Delta) - V(y - M\cos y + \Delta) = \sin y, \quad (106)$$

where $y = \omega t$. Using the properties of parity and periodicity $V(y)$, we seek the solution to functional equation (106) in the form of a series,

$$V(y) = \sum_{n=1}^{\infty} B_n\cos ny, \quad (107)$$

with the unknown coefficients B_n. We obtain,

$$\sum_{n=1}^{\infty} B_n\sin ny\sin n(\Delta - M\cos y) = 0.5\sin y. \quad (108)$$

Now we multiply both sides of (108) by $\sin my$ ($m = 1, 2, 3, \ldots$) and average the obtained correlation over period. As a result, we arrive at a system of equations for determining B_n, which has the form

$$\sum_{n=1}^{\infty} B_n J_n(nM)\cos\left(n\Delta - n\frac{\pi}{2}\right) = \frac{M}{4}, \quad (109)$$

$$\sum_{n=1}^{\infty} B_n\left\{J_{|n-m|}(nM)\sin\left(n\Delta - |n-m|\frac{\pi}{2}\right) - J_{n+m}(nM)\sin\left(n\Delta - (n+m)\frac{\pi}{2}\right)\right\} = 0. \quad (110)$$

In Eqs. (110) it is necessary to suppose that $m = 2, 3, \ldots$, but Eq. (109) corresponds to a value of $m = 1$.

At $M \longrightarrow 0$, system (109), (110) contains an evident transition to the solution to the linear problem: $B_2 = B_3 = \ldots = 0$,

$$B_1 \approx \frac{1}{2\sin\Delta}, \quad V(y) \approx \frac{\cos y}{2\sin\Delta}. \quad (111)$$

Generally, this system can be solved only by numerical methods. An analytical solution can be obtained

only for small values of M and $|\Delta|$; however, it is more convenient to start with functional equation (106), which is approximately combined with the following differential equation:

$$\frac{dV}{dy} = \frac{1}{2}\frac{\sin y}{M\cos y - \Delta}. \quad (112)$$

Its solution at $M < |\Delta|$ has the form

$$V = \frac{1}{2M}\ln\frac{1+\sqrt{1-(M^2/\Delta^2)}}{2[1-(M/\Delta)\cos y]}. \quad (113)$$

The integration constant here is chosen such that the average over period $\bar{V} = 0$.

The form of oscillations V as a function of time $y = \omega t$ is depicted in Fig. 13. The numbers of curves *1–4* correspond to various values of the ratio of small parameters M/Δ of 0.5, 0.7, 0.9, and 0.95. It is clear that at $M/\Delta < 0.5$, the form of oscillations is close to harmonic. As M/Δ approaches unity, nonlinear distortions are manifested even more strongly, leading to the formation of sharp and high positive peaks.

It is important to note that the points of curves in Fig. 13 describe pressure pulsations at the end wall of the resonator, since, according to the second of formulas (88),

$$p(x = L, t)/\rho c^2 = 2MV(\omega t = y). \quad (114)$$

After we find function V (113), it is not difficult to calculate the field of the vibration velocity (88) in the resonator:

$$u = \frac{c}{2}\ln\frac{1-\frac{M}{\Delta}\cos[\omega t + k(x-L)]}{1-\frac{M}{\Delta}\cos[\omega t - k(x-L)]}. \quad (115)$$

The set boundary conditions

$$u(x = L, t) = 0, \quad u(x = -(A/\omega)\cos\omega t, t) = 0 \quad (116)$$

in the solution to (115) are fulfilled, but the second of them is approximate, taking into account the smallness of M and Δ, in the neighborhood of the main resonance $kL = \pi$.

The corresponding (115) field of acoustic pressure is described by the expression

$$p = \rho c^2 \ln\frac{1}{2}\left(1+\sqrt{\frac{M^2}{\Delta^2}}\right) - \frac{\rho c^2}{2} \times \ln\left\{\left[1-\frac{M}{\Delta}\cos(\omega t + k(x-L))\right] \times \left[1-\frac{M}{\Delta}\cos(\omega t - k(x-L))\right]\right\}. \quad (117)$$

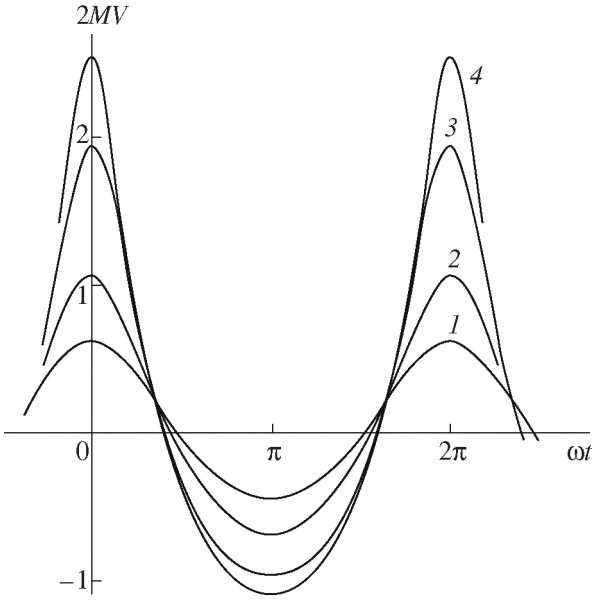

Fig. 13. Form of wall oscillations with time. The numbers of curves *1–4* correspond to ratio values of $M/\Delta = 0.5, 0.7, 0.9, 0.95$. At $M/\Delta < 0.5$, the form is close to harmonic. At $M/\Delta \longrightarrow 1$, nonlinear distortions result in sharp, high positive peaks. The curves describe pulsations in pressure on the closed end wall of the resonator.

The forms of pressure oscillations in various sections of the resonator are depicted in Fig 14. Curves *1–6* correspond to sections x/L equal to 1/6, 1/3, 1/2, 2/3, 5/6, and 1. In order that the curves do not overlap with each other, the first (not depending on t) summand in formula (117) is not taken into account in constructing the graphs. However, it should be remembered that oscillations have a zero constant component and each of curves *1–6* should shift downward along the ordinate axis. As comparison of the curves shows, the temporal forms and spectra of oscillations in various sections of the resonator strongly differ from one another.

The solutions (115) and (117) can be represented in the form of an expansion into series over the harmonics:

$$\begin{pmatrix} u \\ p \end{pmatrix} = \frac{1}{2}\begin{pmatrix} c \\ \rho c^2 \end{pmatrix} \times \sum_{n=1}^{\infty} B_n \begin{pmatrix} \sin(n\omega t)\sin(nk(x-L)) \\ \cos(n\omega t)\cos(nk(x-L)) \end{pmatrix}, \quad (118)$$

where the coefficients of expansion are

$$B_n = \frac{1}{n}\left(\frac{\Delta}{M}\right)^n\left(1-\sqrt{1-\frac{M^2}{\Delta^2}}\right)^n. \quad (119)$$

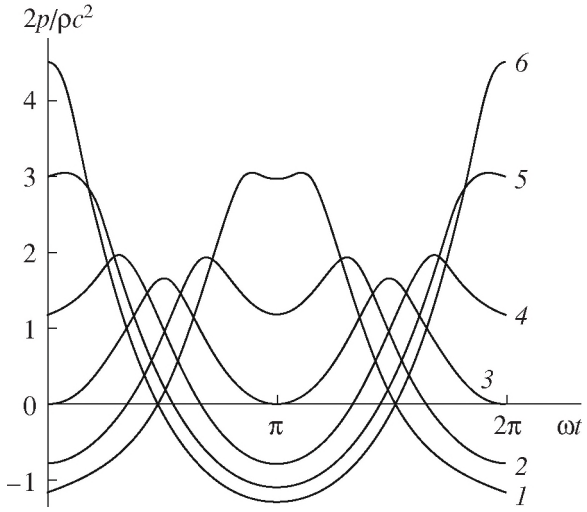

Fig. 14. Form of pressure oscillations in various sections of the resonator. Curves *1–6* correspond to sections *x*/*L* of 1/6, 1/3, 1/2, 2/3, 5/6, and 1.

The energy of oscillations (103) in the neighborhood of the main resonance is

$$E = c^2 L L i_2\left[\left(\frac{\Delta}{M}\right)^2\left(1-\sqrt{1-\frac{M^2}{\Delta^2}}\right)^2\right]; \qquad (120)$$

here, Li_2 is a second-order polylogarithm. The ratio of the energy of nonlinear (120) and linear (103) oscillations at small M/Δ increase with increasing Mach number as

$$\frac{E}{E_{\text{lin}}} \approx 1 + \frac{1}{8}\left(\frac{M}{\Delta}\right)^2. \qquad (121)$$

At $M/\Delta \longrightarrow 1$, this ratio tends to $2\pi^2/3$.

In conclusion, we estimate the possibility of the described effects of boundary nonlinearity. The condition $M/\Delta \sim 1$ is equivalent to

$$(2I/c^3\rho)^{1/2} Q \sim 1, \qquad (122)$$

where I is the intensity of the source exciting the resonator. Clearly, condition (122) is fulfilled for a resonator with a Q-factor of $Q \sim 10^4$ if the intensity $I \sim 2$ W/cm^2 (here ρ and c are assumed the same as in water).

The estimate shows that the boundary nonlinearity probably manifested itself in experiments conducted earlier. However, we do not know if these phenomena have been observed in "pure" form, whereas in hi-Q resonators it was possible to exclude the background of volume effects and focus attention on the effects of boundary nonlinearity.

The problem on approaching resonance, in the proximity of which the ratio $M > |\Delta|$ remains open. In the steady-state solution, particular features arise; therefore it is necessary to analyze the establishment of oscillations. It is interesting also to take into account in a competing factor—weak loss owing to linear dissipation. We turn now to a discussion of the above-mentioned problems.

Proceeding from Eq. (24), in which we consider the movement of a wall harmonic, $\Phi(\xi) = \cos\xi$, and we ignore volume nonlinearity, supposing that $\varepsilon = 0$:

$$\frac{\partial U}{\partial T} - M\cos\xi\frac{\partial U}{\partial \xi} + \Delta\frac{\partial U}{\partial \xi} - D\frac{\partial^2 U}{\partial \xi^2} = -\frac{M}{2}\sin\xi. \qquad (123)$$

If we ignore movement of the boundary, that is, the second term in the left-hand side of Eq. (123), it is not difficult to obtain formulas that describe the process of establishment of linear oscillations corresponding to the zero initial condition—$U(T = 0, \xi) = 0$:

$$U = B(T)\cos[\xi + \varphi(T)],$$

$$B = \frac{M}{2}\left[\frac{1 - 2\exp(-DT)\cos\Delta T + \exp(-2DT)}{\Delta^2 + D^2}\right]^{1/2}, \qquad (124)$$

$$\varphi(T) = \arctan\frac{D}{\Delta} + \arctan\left[\frac{\exp(-DT)\sin\Delta T}{1 - \exp(-DT)\cos\Delta T}\right].$$

At small T, solution (124) describes the beginning of the process of establishment and linear increase in amplitude: $U \approx -(MT/2)\sin\xi$. At $T \longrightarrow \infty$, the solution (124) tends to the steady-state form:

$$U \approx \frac{M}{2\sqrt{\Delta^2 + D^2}}\cos\left(\xi + \arctan\frac{D}{\Delta}\right). \qquad (125)$$

Now, proceeding from Eq. (123), we solve the direct and inverse problems. The simpler inverse problem consists in finding the law of boundary motion resulting in the establishment of the given wave form in the resonator. One of its solutions,

$$M\Phi(\xi) = kX(\xi - \pi) = \Delta\left[1 - \frac{\exp\left(-\frac{M}{\Delta}\exp(-DT)\cos\xi\right)}{I_0\left(\frac{M}{\Delta}\exp(-DT)\right)}\right], \qquad (126)$$

$$U = \frac{M}{2\Delta}\exp(-DT)\cos\xi,$$

in the presence of attenuation ($D = 0$) coincides in its form with formula (96). In contrast to formula (96), solution (126) is non-steady-state. It describes the transition from the strongly nonlinear (for values of $M/\Delta \gg 1$) regime of wall oscillations to purely harmonic linear oscillations (at $T \longrightarrow \infty$) occurring as a result of dissipation. Despite the complex form of wall oscillations,

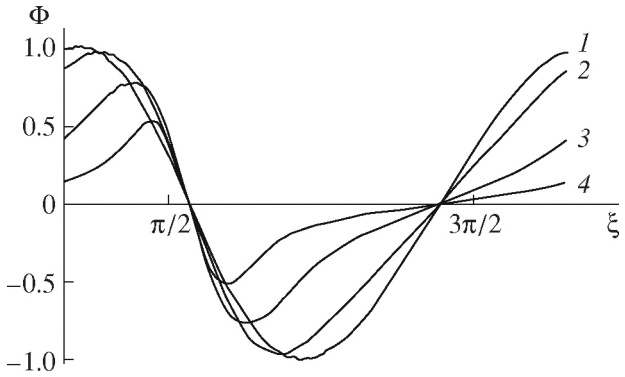

Fig. 15. Law of wall movement causing linear oscillations in the resonator. Values of detuning, dissipation parameter, and slow time are chosen, respectively, as $\Delta = 0$; $D = 0.01$; and $T = 10^{-1}, 1, 10, 10^2$. At small T, movement is almost harmonic. At large T, the boundary moves in a complex way.

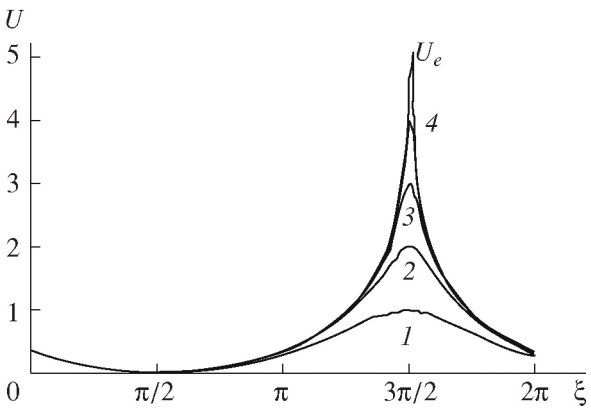

Fig. 16. Process in which a wave profile $U(T, \xi)$ is established for small detunings. Moments of time $T = 10$, 20, 30, 40 for values of parameter $\Delta = 0$, $M = 0.1$ are examined.

the oscillations in the layer remain harmonic at any moment of time; at $T \longrightarrow \infty$ they also attenuate.

We now find the law of periodic movement of a wall leading to the formation of linear (nonattenuating at $T \longrightarrow \infty$ oscillations (124) in the resonator. Proceeding from the fact that (124) satisfies the equation

$$\frac{\partial U}{\partial T} + \Delta\frac{\partial U}{\partial \xi} + DU = -\frac{M}{2}\sin\xi, \tag{127}$$

and subtracting (127) from (123), we obtain the equation for function $\Phi(\xi)$:

$$d\Phi/d\xi = 2\Phi\sin(\xi + \varphi) - \sin\xi. \tag{128}$$

The solution to Eq. (128), which corresponds to a zero average value for the period, is shown in Fig. 15. The following parameters have been chosen: $\Delta = 0$, $D = 0.01$, $T = 10^{-1}, 10^0, 10, 10^2$. It is clear from the figure that at small values of time T, movement of the wall is almost harmonic; at large T, the boundary should complete a quite complex movement.

We now pass to solving the direct problem for determining the wave form according to the given law of movement of the wall of a resonator. If we do not take into account dissipation, it is necessary to solve the equation

$$\frac{\partial U}{\partial T} + (\Delta - M\cos\xi)\frac{\partial U}{\partial \xi} = -\frac{M}{2}\sin\xi. \tag{129}$$

The solution to (129), which is periodic in ξ and satisfies the zero initial condition $U(T = 0, \xi) = 0$, takes the form

$$U = -\frac{1}{2}\ln[A(T)\cos\xi + B(T)\sin\xi + C(T)],$$

$$A = \frac{M\Delta}{M^2 - \Delta^2}[1 - \cosh(T\sqrt{M^2 - \Delta^2})],$$
$$B = \frac{M}{\sqrt{M^2 - \Delta^2}}\sinh(T\sqrt{M^2 - \Delta^2}), \tag{130}$$
$$C = \frac{M^2\cosh(T\sqrt{M^2 - \Delta^2}) - \Delta^2}{M^2 - \Delta^2}$$

for small detunings when $\Delta^2 < M^2$, and the same form with different functions

$$A = \frac{M\Delta}{\Delta^2 - M^2}[\cos(T\sqrt{\Delta^2 - M^2}) - 1],$$
$$B = \frac{M}{\sqrt{\Delta^2 - M^2}}\sin(T\sqrt{\Delta^2 - M^2}), \tag{131}$$
$$C = \frac{\Delta^2 - M^2\cosh(T\sqrt{\Delta^2 - M^2})}{\Delta^2 - M^2}$$

for detunings $\Delta^2 > M^2$.

We will discuss formulas obtained in [15, 16]. For small detunings $|\Delta| < M$, the expression under logarithm (130) is positively determined and a solution at finite T has no singularities. At $T \longrightarrow \infty$, it takes the form

$$U = -\frac{1}{2}\ln S, \tag{132}$$
$$S = \frac{\exp(M\sin\xi_* T)}{\sin^2\xi_*}\sin^2\frac{\xi + \xi^*}{2}, \quad \sin\xi_* \equiv \sqrt{1 - \frac{\Delta^2}{M^2}}.$$

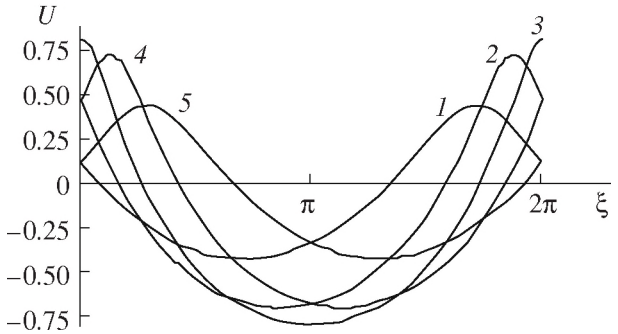

Fig. 17. Process in which a wave profile $U(T, \xi)$ is established for large detunings $|\Delta| > M$. Parameters $\Delta = 0.15$, $M = 0.1$. Moments of time $T = 2\pi n/6\sqrt{\Delta^2 - M^2}$, $n = 1, 2, 3, 4, 5$ are chosen.

The form of the established wave (132) has a logarithmic singularity at $\xi = -\xi_*$. We introduce the notation

$$U_e(\xi) = \lim_{T\to\infty}\left[U(T,\xi) + \frac{1}{2}MT\sin\xi_*\right] = \ln\sin\xi_* - \ln\sin\frac{\xi+\xi_*}{2}. \quad (133)$$

Figure 16 shows the graphs of function (133) at moments of time $T = 10, 20, 30, 40$ for values of the parameters of $\Delta = 0$, $M = 0.1$. It is seen to that at point $\xi = -\xi_*$ in the wave profile, a sharp peak forms, the value of which increases with time. Clearly, growth of the peak is limited by dissipation and at $T \longrightarrow \infty$, it is necessary to take into account the term $D\partial^2 U/\partial\xi^2$, discarded in passing from Eq. (123) to (129). The solution to the problem with small dissipation by means of matched asymptotic expansions has given the following results. The peak value of perturbation in the established wave profile takes a finite value.

$$U_{\max} = \eta + \ln\left(2\sqrt{\frac{M}{D}}\sin^{3/2}\xi_*\right),$$
$$\eta = \lim_{y\to\infty}\left[\sqrt{2}\ln\int_0^y F\left(\frac{x}{\sqrt{2}}\right)dx - \ln y\right] \approx 0.635. \quad (134)$$

The time it takes for steady-state oscillations to form in the resonator is estimated by the formula

$$T_{ST} \sim \frac{1}{M\sin\xi_*}\ln\left(\sqrt{\frac{M}{D}}\sin^{3/2}\xi_*\right). \quad (135)$$

We draw attention to the fact that in a normal resonator (without absorption and nonlinearity), unlimited growth in the amplitude in time is observed when excitation frequencies and eigenfrequencies coincide ($\Delta = 0$). When we take into account the finiteness of movement of the boundary, such resonance behavior occurs not only at $\Delta = 0$, but also in the range of detunings $|\Delta| < M$. In addition, the wave form is essentially nonharmonic. Figure 16 shows that many high harmonics appear in the spectrum.

In the second case, for large detunings $|\Delta| > M$, there are no singularities and the solution takes the form of (131). The wave profiles $U(T, \xi)$ for values of the parameters of $\Delta = 0.15$, $M = 0.1$ are depicted in Fig. 17. Moments of time $T = 2\pi n/6\sqrt{\Delta^2 - M^2}$, $n = 1, 2, 3, 4, 5$ have been chosen. Clearly, "beats" are observed the frequency of which depends on the normalized amplitude M of wall oscillations. The frequency decreases at $M \longrightarrow |\Delta|$.

A RESONATOR FILLED WITH A CUBIC NONLINEAR MEDIUM

Cubic nonlinear systems have been studied to a far lesser extent. They are interesting for two reasons. First, it is a novel object the evolution of which significantly differs from the evolution of a quadratic nonlinear wave. This problem has been studied as applied to the basic theory of nonlinear waves in media without dispersion, for plane waves [30] non-1D beams [31]. Second, cubic nonlinear media are very interesting in connection to new applied problems. One group of such problems deal with excitation of strong shear waves for medical purposes [32–34]; another group deals with various geophysical applications [35]. New data have appeared on measuring the cubic nonlinearity of such media as rubber and phantom biological tissue [34].

As shown above, success in studying standing waves in ordinary quadratic nonlinear resonators has been achieved with the help of an approximation that supposes the superposition of two nonlinear waves traveling toward each other. A similar approach can be applied to a cubic resonator, but the idea of full independence of opposing waves is now erroneous.

In order to show how it is possible to modify these ideas, we examine a wave equation that models shear waves in any homogeneous solid body (cf. Eq. (1)):

$$\frac{\partial^2 u}{\partial x^2} - \frac{1}{c^2}\frac{\partial^2 u}{\partial t^2} = -\frac{2\varepsilon}{3c^4}\frac{\partial^2 u^3}{\partial t^2}. \quad (136)$$

Using the method of a slowly changing profile [14], we can deduce from (136) a simplified evolutionary first-order equation,

$$\frac{\partial u}{\partial x} - \frac{\varepsilon}{c^3}u^2\frac{\partial u}{\partial \tau} = 0, \quad (137)$$

for simple (Riemann) waves traveling in cubic nonlinear media. Here $\tau = t - x/c$; x is the slow coordinate [14].

The properties of cubic nonlinear Riemann waves have been studied in [30]. It is shown that progressive distortion of the initial harmonic wave leads to the formation of an asymmetrical time profile. During further

propagation in the profile, discontinuities appear. In contrast to a quadratic nonlinear wave, which contains only compression shocks, each period of the wave in a cubic medium contains both a compression shock front and an expansion shock front. A cubic nonlinearity changes the velocity of propagation; for acoustic beams, a change in the velocity in a cross section leads to the appearance of self-focusing and defocusing phenomena [31, 36, 37].

We seek the solution to Eq. (136) in the following form:

$$u = u_+\left(x_1 = \mu x, \tau_+ = t - \frac{x}{c}\right) + u_-\left(x_1 = \mu x, \tau_- = t + \frac{x}{c}\right). \quad (138)$$

Here, $\mu \ll 1$ is a small parameter of the problem; for a cubic nonlinear wave, it is on the order of the acoustic Mach number squared ($\sim \varepsilon u_{\max}^2/c^2$). After substituting (138) into (136) and neglecting terms on the order of μ^2, μ^3, it is possible to obtain

$$\left(-\frac{2\varepsilon}{3c^4}\right)^{-1}\left(-\frac{2}{c}\frac{\partial^2 u_+}{\partial x \partial \tau_+} + \frac{2}{c}\frac{\partial^2 u_-}{\partial x \partial \tau_-}\right) = \frac{\partial^2 u_+^3}{\partial \tau_+^2} + 3\frac{\partial^2 u_+^2}{\partial \tau_+^2}u_- + 3u_+^2\frac{\partial^2 u_-}{\partial \tau_-^2} + 6\frac{\partial u_+^2}{\partial \tau_+}\frac{\partial u_-}{\partial \tau_-} + 3\frac{\partial^2 u_+}{\partial \tau_+^2}u_-^2 + 3u_+\frac{\partial^2 u_-^2}{\partial \tau_-^2} + 6\frac{\partial u_+}{\partial \tau_+}\frac{\partial u_-^2}{\partial \tau_-} + \frac{\partial^2 u_-^3}{\partial \tau_-^2}.$$

Let u_+ be a rapidly oscillating function of variable τ_+ and, analogously, u_- be a rapidly oscillating function of variable τ_-. Let the average period values be equal to zero: $\langle u_+\rangle_{\tau_+} = \langle u_-\rangle_{\tau_-} = 0$. Averaging the latter expression subsequently over the variables τ_- and τ_+, we obtain the following system [38, 39]:

$$\frac{\partial u_+}{\partial x} - \frac{\varepsilon}{c^3}(\langle u_-^2\rangle + u_+^2)\frac{\partial u_+}{\partial \tau_+} = 0, \quad (139)$$

$$\frac{\partial u_-}{\partial x} + \frac{\varepsilon}{c^3}(\langle u_+^2\rangle + u_-^2)\frac{\partial u_-}{\partial \tau_-} = 0. \quad (140)$$

Equations (139) and (140), in contrast to analogous equations for a quadratic nonlinear medium, are not independent. They are connected through the mean squares (mean intensities) $I_+ = \langle u_+^2\rangle \neq 0$, $I_- = \langle u_-^2\rangle \neq 0$ of variables u_+, u_-. For standing waves, clearly it is necessary to suppose $I_+ = I_- = I$.

With the method described above for quadratic nonlinearity (see (4)–(7)), it is not difficult to check that all discarded terms are nonresonant and cannot significantly affect the exchange of the energy between the harmonics of two waves traveling toward each other.

It is possible to represent the nonlinear field in a resonator as the sum of two exact solutions to Eqs. (139) and (140) by analogy with the representation for the problem with quadratic nonlinearity. We write these two solutions in a form convenient for us:

$$u_+ = F_+\left[\omega t - k(x-L) + \frac{\varepsilon}{c^2}k(x-L)(I+u_+^2)\right],$$
$$u_- = F_-\left[\omega t + k(x-L) - \frac{\varepsilon}{c^2}k(x-L)(I+u_-^2)\right]. \quad (141)$$

Here, $k = \omega/c$ is the wavenumber and $x = L$ is the coordinate of the right boundary of the nonlinear medium occupying the area of $0 < x < L$. Functions F_+, F_- are determined from boundary conditions.

As is known, during excitation of a field by a harmonic source at frequency ω in a cubic medium, only odd harmonics with frequencies of $(2n + 1)\omega$ are excited. If ω is close to the frequency of the main mode ω_1, then pure standing waves can form only in the case when the frequencies of the higher harmonics are close to the frequencies of the corresponding higher modes. Such a regime is the most interesting, since it makes it possible to accumulate significant energy in the cavity of the resonator even when there is a weak external source.

A resonator with the needed spectrum,

$$\omega_{2n+1} = (2n+1)\omega_1, \quad \omega_1 = \frac{\pi c}{2L}, \quad n = 0, 1, 2\ldots, \quad (142)$$

has one wall (for instance, $x = 0$) that is rigid with $u(x = 0, t) = 0$ on it; on the second wall, the velocity of oscillations has a maximum, that is,

$$\left.\frac{\partial u}{\partial x}\right|_{x=L} = \left(\frac{\partial u_+}{\partial x} + \frac{\partial u_-}{\partial x}\right)_{x=L} = 0. \quad (143)$$

From boundary condition (143), we find that arbitrary functions F_+, F_- in the solution to (141) should be the same, $F_+ = F_- = F$. As well, the field in the resonator is written as follows:

$$u = F\left[\omega t - \frac{\omega}{c}(x-L) + \frac{\varepsilon\omega}{c^3}(I+F^2)(x-L)\right] + F\left[\omega t + \frac{\omega}{c}(x-L) - \frac{\varepsilon\omega}{c^3}(I+F^2)(x-L)\right]. \quad (144)$$

Let the border $x = 0$ oscillate according to the harmonic law

$$u(x = 0, t) = A\sin(\omega t). \quad (145)$$

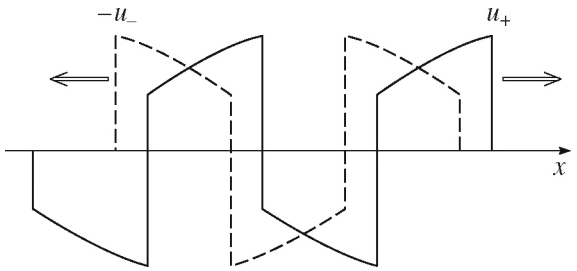

Fig. 18. Form of wave profiles for waves traveling toward each other in a cubic nonlinear medium.

Using (145), we reduce (144) to the nonlinear functional equation

$$F\left[\omega t + kL - \frac{\varepsilon}{c^2}kL(I+F^2)\right] + F\left[\omega t - kL + \frac{\varepsilon}{c^2}kL(I+F^2)\right] = A\sin(\omega t). \quad (146)$$

If we linearize Eq. (146), formally setting $\varepsilon = 0$, we can find its general solution:

$$F = \frac{A\sin(\omega t)}{2\cos(kL)} + \sum_{n=0}^{\infty}[A_{2n+1}\cos(2n+1)\omega_1 t + B_{2n+1}\sin(2n+1)\omega_1 t]. \quad (147)$$

When there is exact resonance, for instance, in the main mode $\omega = \omega_1$, solution (147) describes oscillations infinitely increasing in time according to the linear law

$$F = -\frac{A}{\pi}(\omega_1 t)\cos(\omega_1 t). \quad (148)$$

As is known, this increase is limited by absorption, nonlinearity, or detuning of the frequency from exact resonance:

$$kL = \frac{\pi}{2} + \Delta, \quad \Delta = (\omega - \omega_1)\frac{L}{c} = \frac{\pi(\omega-\omega_1)}{2\omega_1} \ll 1. \quad (149)$$

Here and further, dimensionless detuning Δ is considered a small value. Taking into account $\Delta \neq 0$, oscillations appear to be modulated; they are described by a function limited in time:

$$F = -A\sin^{-1}\left(\frac{\pi}{2}\frac{\omega-\omega_1}{\omega_1}\right) \times \sin\left(\frac{\omega-\omega_1}{2}t\right)\cos\left(\frac{\omega+\omega_1}{2}t\right). \quad (150)$$

Using the method described in [21], we reduce functional equation (143) to the differential equation

$$\frac{\partial U}{\partial T} + \left(\Delta - \frac{\pi\varepsilon}{2}J - \frac{\pi\varepsilon}{2}U^2\right)\frac{\partial U}{\partial \xi} - D\frac{\partial^2 U}{\partial \xi^2} = -\frac{M}{2}\cos\xi. \quad (151)$$

For simplicity in writing and comparing the results, here we use the same dimensionless notations as in [21]:

$$U = \frac{F}{c}, \quad M = \frac{A}{c}, \quad J = \frac{I}{c^2}, \quad \xi = \omega t + \frac{\pi}{2}, \quad T = \frac{\omega t}{\pi}, \quad D = \frac{b\omega^2}{2c^3\rho}L. \quad (152)$$

The dissipative term with the second derivative is introduced into Eq. (151) in accordance with the procedure described earlier in [21]. Parameter D is also a small value; it is proportional to the effective viscosity b and equal to the product of the coefficient of absorption of the wave by the length of the resonator L. In Eq. (151), we use two time variables: fast time ξ and slow time T. Slowness T is provided by the smallness of three coefficients in Eq. (151), namely: Δ, D, and $M \sim U$ (see also [21]).

It is expedient to begin the analysis of standing waves by examining the very simple case of free oscillations. Let the left boundary of the resonator be immobile; therefore, the velocity on it is equal to zero, $u(x, t) = 0$, at $x = 0$. On the right boundary, $x = L$, the derivative is equal to zero, $\partial u/\partial x = 0$. At the initial moment of time $t = 0$, large-amplitude oscillations arise between the immobile walls. Further evolution of the acoustic field takes place without inflow of additional energy from outside.

This problem is solved on the basis of the approach described above for quadratic nonlinearity. As well, instead of inhomogeneous equation (151), for the auxiliary function U it is necessary to solve a homogeneous ($M = 0$) equation. The results of analysis of a homogeneous equation corresponding to (151) are known and described in detail [30, 31] for propagating perturbations. However, as shown above, it is possible to construct a standing wave as the sum of two waves traveling toward each other. This procedure is explained in Fig. 18.

We see that each of the two initially harmonic waves over the course of a long time takes on a saw-tooth shape. However, in contrast to a quadratic nonlinear medium, every tooth (half-period) now has not a triangular, but a trapezoidal form. The peak of the positive vibration velocity on the forward compression jump exceeds the module of the negative value of this jump by a factor of 2. On the other hand, the module of the negative value on the expansion jump is twice as large as the positive value.

Using the idea of linear superposition of two waves strongly distorted by cubic nonlinearity, we can con-

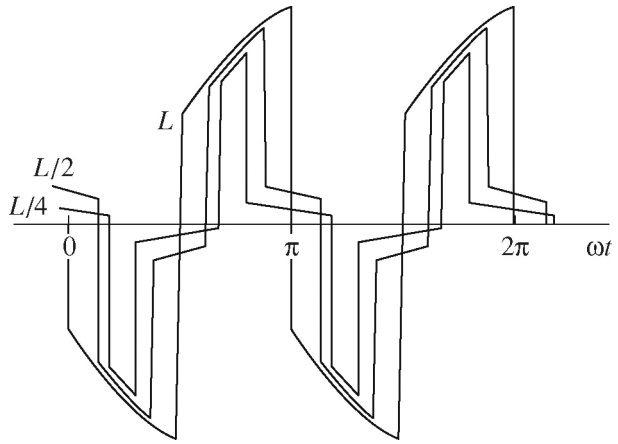

Fig. 19. Form of a standing wave with time, measured in various sections of the resonator at distances of $L/4$, $L/2$, L from the left end wall.

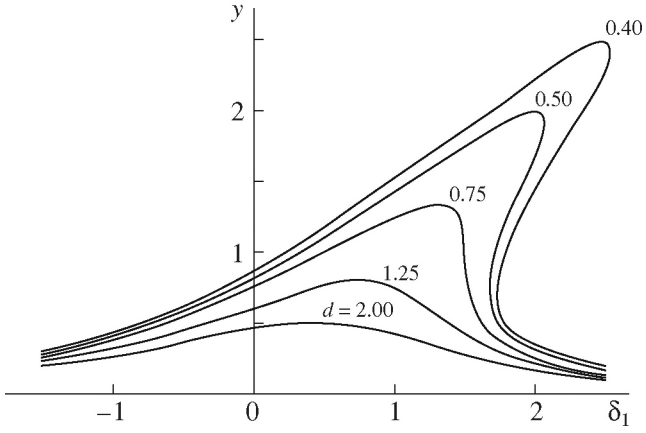

Fig. 20. Resonance curves for the mean oscillation intensity in a cubic nonlinear resonator for various values of dissipation parameter d.

struct the profiles of standing waves by a formula that follows from (144):

$$\frac{u}{c} = U[\omega t - k(x - L)] + U[\omega t + k(x - L)]. \quad (153)$$

Here, U describes the distorted profile of a wave traveling in a positive or negative direction along the x axis. The arguments of both functions U in formula (153) do not contain nonlinear terms, because the profiles are constructed in the limits of one period of oscillations. Here it is necessary to recall that nonlinear effects are capable of accumulating and significantly distorting the profile over the course of many periods. The number of them is proportional to $(\varepsilon M^2)^{-1} \gg 1$ (see, e.g., [1]).

The time profiles measured in various sections of the resonator, equal to $L/4$, $L/2$, L, are shown in Fig. 19. We see that two narrow impulses in velocity (positive and negative) form as the section approaches the left end of the resonator. Upon reaching the wall $x = 0$, these peaks disappear and the velocity here goes to zero.

We now look at induced standing waves. In contrast to the homogeneous equation, the full version of inhomogeneous equation (151) has not been studied and there are no fundamental results for traveling waves that could possibly be adapted to describe standing waves.

The first attempt at analysis here deals with a very simple method of harmonic balance, which is well known in the theory of vibrations. According to this method, it is necessary to seek a weakly nonlinear solution to Eq. (151) in the form

$$U = A(T)\cos\xi + B(T)\sin\xi. \quad (154)$$

Singling out terms standing for functions $\sin\xi$, $\cos\xi$, we obtain a system of two coupled ordinary differential equations:

$$\frac{dB}{dT} - \left[\Delta - \frac{3\pi\varepsilon}{8}(A^2 + B^2)\right]A + DB = 0,$$
$$\frac{dA}{dT} + \left[\Delta - \frac{3\pi\varepsilon}{8}(A^2 + B^2)\right]B + DA = -\frac{M}{2}. \quad (155)$$

It is not difficult to analyze this system by numerical methods. However, an analytical solution exists that corresponds to the regime of oscillations being established. This solution is achieved at $T \longrightarrow \infty$, when the time derivatives in (155) go to zero: $dA/dT = dB/dT = 0$. The steady-state solution to (155) looks as follows:

$$\left[\Delta - \frac{3\pi\varepsilon}{8}(A^2 + B^2)\right]^2 + D^2 = \frac{M^2}{4}(A^2 + B^2)^{-1}. \quad (156)$$

This solution is written in a very simple form,

$$\delta_1 = y \pm \sqrt{y^{-1} - d^2}, \quad (157)$$

using the following notations:

$$\delta_1 = \frac{\Delta}{C}, \quad d = \frac{D}{C}, \quad y = \frac{3}{4}\pi\varepsilon\frac{J}{C},$$
$$C = \left(\frac{3\pi\varepsilon M^2}{32}\right)^{1/3}, \quad J = \frac{1}{2}(A^2 + B^2). \quad (158)$$

The resonance curves for the mean intensity $y(\delta_1)$ are shown in Fig. 20 for various values of the dissipation parameter of $d = 2.00$, 1.25, 0.75, 0.50, 0.40. With strengthening absorption, the curve of the frequency response is distorted in shape. When there is weak absorption, $d < \sqrt{3}/2$, this curve describes an multiple-valued function in a certain area of positive values of δ_1.

We now look at induced waves with discontinuities. Solution (156) has been obtained by the method of harmonic balance (154). Its accuracy is low for strongly distorted waves, especially in the most interesting case

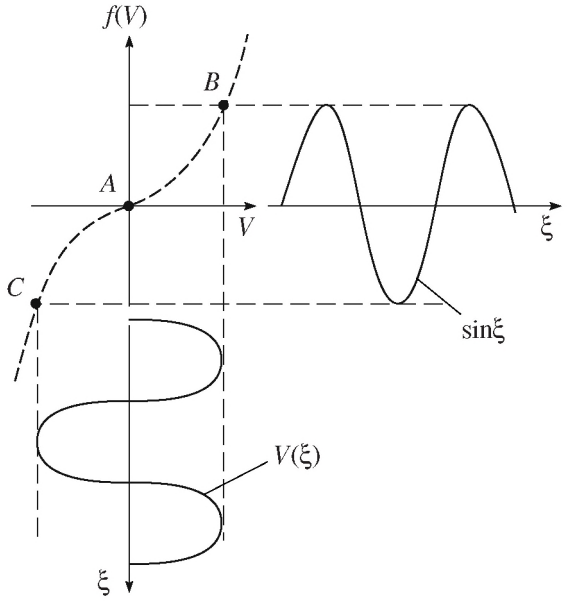

Fig. 21. Analysis of the wave profile in graph form. Curve $f(V)$ is shown by the dashed line, along which the vertical projection of function $\sin\xi$ moves. Movement begins at moment $\xi = 0$ at point A; after that, oscillations occur between points B and C.

when the wave profile contains shock fronts. Therefore, using another approach, we will look at induced waves described by Eq. (151). The steady-state regime, achieved in the limit case $T \longrightarrow \infty$, is described by an ordinary differential equation that follows from (151):

$$\left(\Delta - \frac{\pi\varepsilon}{2}J - \frac{\pi\varepsilon}{2}U^2\right)\frac{dU}{d\xi} - D\frac{d^2U}{d\xi^2} = -\frac{M}{2}\cos\xi. \quad (159)$$

After integration of (159) taking into account condition $\langle U\rangle = 0$, we obtain the first-order equation

$$D\frac{dU}{d\xi} + \frac{\pi\varepsilon}{6}U^3 + \left(\frac{\pi\varepsilon}{2}J - \Delta\right)U = \frac{M}{2}\sin\xi. \quad (160)$$

For simplification of the subsequent formulas, we introduce the new notations

$$V = U\left(3\frac{M}{\pi\varepsilon}\right)^{-1/3}, \quad j = J\left(3\frac{M}{\pi\varepsilon}\right)^{-2/3},$$
$$\Gamma = D\left(\frac{\pi\varepsilon}{24}M^2\right)^{-1/3}, \quad \delta = \frac{\Delta}{3}\left(\frac{\pi\varepsilon}{24}M^2\right)^{-1/3}, \quad (161)$$

which differ somewhat from the earlier used notations of (158). Thus, the mean intensities j and y differ in their numerical multiplier on the order of unity just like other pairs: the limitless dissipative coefficients Γ and d, and normalized detunings δ and δ_1. These differences are a result of considerations of simplicity. The notations of (158) make it possible to write solutions (155), (156) in a very simple form; at the same time, the notations of (161) make it possible to bring Eq. (160) to the following form:

$$\Gamma\frac{dV}{d\xi} + V^3 + 3(j-\delta)V = \sin\xi. \quad (162)$$

Clearly, weakly absorbing media are the most interesting, since nonlinear phenomena in such media can be strongly expressed. In order to describe the wave profile in a perfect medium without dissipation, we set $\Gamma = 0$ in Eq. (162). As is shown below, the approximation $\Gamma \longrightarrow 0$ is everywhere correct, with the exception of a small neighborhood of shock fronts. This approximation corresponds to neglecting the derivative, which turns differential equation (162) into an algebraic equation. However, this new equation,

$$f(V) = V^3 + 3(j-\delta)V = \sin\xi, \quad (163)$$

is not a usual cubic equation, because its solution should satisfy the additional integral conditions

$$\langle V\rangle = \frac{1}{2\pi}\int_0^{2\pi} V d\xi = 0, \quad \langle V^2\rangle = \frac{1}{2\pi}\int_0^{2\pi} V^2 d\xi = j. \quad (164)$$

Therefore, constant j in Eq. (163) is not known a priori; it is necessary to determine it only after we find the solution to (163) with an arbitrary value of j.

Here various situations are possible, and we will examine them individually.

1. Let the mean intensity be larger that the detuning, i.e., $j - \delta \equiv a^2 > 0$. Equation (163) for this case takes the form

$$f(V) = V^3 + 3a^2V = \sin\xi. \quad (165)$$

The qualitative behavior of the solution is shown in Fig. 21. The form of the solution in time (the wave profile) is found simply by constructing a graph. First, in accordance with the equation $f(V) = \sin\xi$, an illustrative point is found that slips with increasing time ξ along the curve $f(V)$ in the cycle $A \longrightarrow B \longrightarrow C \longrightarrow A$. Second, the horizontal projection of the motion of this point is constructed, which gives the wave profile $V(\xi) = f^{-1}[V(\xi)]$, where f^{-1} is the inverse function with respect to function f.

Clearly, profile $V(\xi)$ for this case has no singularity, since function $f(V)$ is monotonic. The period and polarity of $V(\xi)$ are the same as in the right-hand side of Eq. (165), formed by function $\sin\xi$. Of course, wave $V(\xi)$ is distorted; its spectrum contains higher harmonics, because the graph of function $f(V) = V^3 + 3a^2V$ is not a straight line. The difference between $V(\xi)$ and $\sin\xi$, which manifests itself in nonlinear distortion of the wave, strengthens with increasing oscillation amplitude.

2. Let the mean intensity be equal to the detuning, i.e., $j - \delta = 0$.

Equation (163) for this case,

$$f(V) = V^3 = \sin\xi, \quad (166)$$

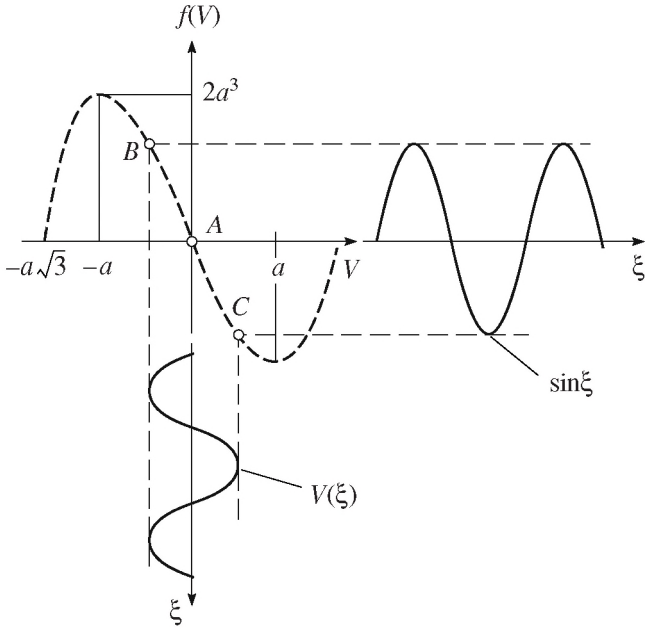

Fig. 22. Analysis of the wave profile in graph form (by analogy to Fig. 21) for large positive detunings $\delta = j + a^2$ in the case of $2a^3 > 1$.

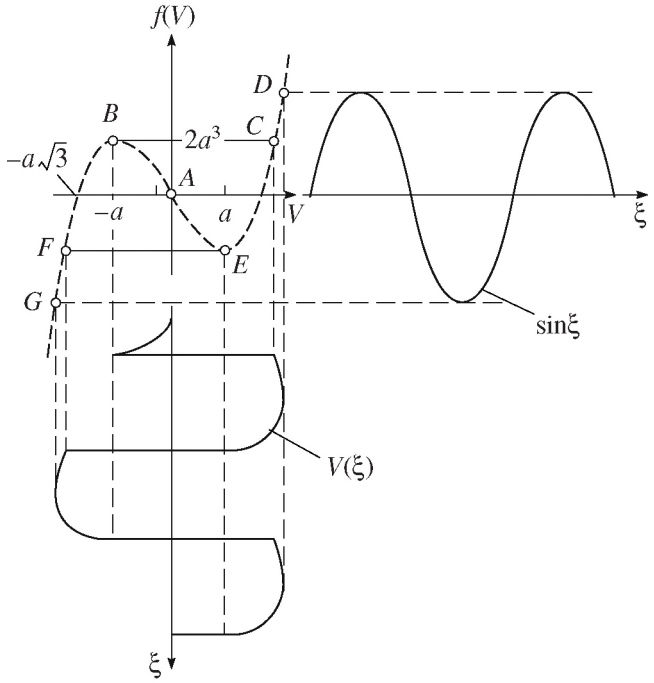

Fig. 23. Analysis of the wave profile in graph form (by analogy to Fig. 22) for large positive detunings $\delta = j + a^2$ in the case of $2a^3 < 1$.

has an exact analytical solution:

$$V = \sin^{1/3}(\xi) = \sum_{n=1}^{\infty} B_{2n-1}\sin[(2n-1)\xi],$$
$$j = \frac{1}{\sqrt{\pi}}\Gamma\left(\frac{5}{6}\right) \approx 0.64. \tag{167}$$

Expansion into Fourier series contains only odd harmonics with amplitudes of

$$B_{2n-1} = \frac{3}{2^{4/3}}\frac{\Gamma(7/3)}{\Gamma(2/3+n)\Gamma(5/3-n)},$$
$$B_{2n} = 0, \quad n = 1, 2, 3, \ldots. \tag{168}$$

Obviously, there are no even harmonics in this expansion, since the nonlinearity of the medium is not quadratic, but cubic.

Numerical estimate (167) points to an upper limit for the case $j - \delta > 0$. Clearly, the increase in detuning in the limits of the interval $-\infty < \delta < 0.64$ leads to an increase in intensity from zero to 0.64.

3. Let a positive detuning be larger that the mean intensity, i.e., $j - \delta \equiv -a^2 < 0$, and in addition, $2a^3 > 1$. Equation (163) for this case is

$$f(V) = V^3 - 3a^2V = \sin\xi. \tag{169}$$

The behavior of the solution to (169) is analyzed in Fig. 22. We see that oscillations of the right-hand side of Eq. (169) lead to movement of the illustrative point in the cycle $A \longrightarrow B \longrightarrow C \longrightarrow A$ along the curve $f(V)$. Analogously to case 1, the wave profile $V(\xi)$ is distorted by nonlinearity, but it does not contain discontinuities. The polarity of oscillations in function $V(\xi)$ are inverse in relation to $\sin\xi$, in contrast to the profile shown in Fig. 21.

4. Let a positive detuning be greater than the mean intensity, $j - \delta \equiv -a^2 < 0$, but $2a^3 < 1$. This case is the most difficult for analysis because discontinuities arise in certain sectors of the wave profile.

We study Eq. (169), supposing that $0 < 2a^3 < 1$. As well, algebraic equation (169) has one real root for $|\sin\xi| > 2a^3$ and three real roots for $|\sin\xi| < 2a^3$. Supposing that $2a^3 < \sin\xi < 1$, we find the single root V_1:

$$V_1 = \sqrt[3]{0.5\sin\xi + 0.5\sqrt{\sin^2\xi - 4a^6}} + \sqrt[3]{0.5\sin\xi - 0.5\sqrt{\sin^2\xi - 4a^6}}. \tag{170}$$

For values of $0 < \sin\xi < 2a^3$, we find the three real roots

$$V_1 = 2a\cos f(\xi), \quad f(\xi) \equiv \frac{1}{3}\arccos\frac{\sin\xi}{2a^3} \tag{171}$$

$$V_2 = -a\cos f(\xi) - \sqrt{3}a\sin f(\xi), \tag{172}$$

$$V_3 = -a\cos f(\xi) + \sqrt{3}a\sin f(\xi). \tag{173}$$

From Eq. (169) it follows that the solution should change sign if function $\sin\xi$ becomes negative.

To qualitatively construct the form of the wave profile, we turn to Fig. 23. Let movement begin at point A from a value of $V = 0$ at $\xi = 0$. From expressions (171)–(173) we find that at $\xi = 0$ there are three roots: $V_1 = a\sqrt{3}$, $V_2 = -a\sqrt{3}$, $V_3 = 0$. Clearly, when the argument ξ increases in the area of $0 \le \xi < \xi_S$, which is denoted $\sin\xi_S = 2a^3$, it is necessary to choose the third root $V = V_3$.

When the argument achieves a value of $\xi = \xi_S$, the solution changes jumpwise from a value of $V = V_3(\xi_S) = -a$ to $V = V_1(\xi_S) = 2a$, which corresponds to a jump from state B to state C. In sector CD there is a unique real solution $V = V_1$ to (170), which attains a maximum at point D at $\xi = \pi/2$:

$$V(\pi/2) = V_1(\pi/2) = \sqrt[3]{0.5 + 0.5\sqrt{1 - 4a^6}} + \sqrt[3]{0.5 - 0.5\sqrt{1 - 4a^6}}. \quad (174)$$

With further growth of variable ξ, it crosses through $\xi = \pi - \xi_S$ and solution V_1 changes its analytical representation from (170) to (171).

With a value of the argument of $\xi = \pi$, function $\sin\xi$ changes its sign and root V_1, as follows from Eq. (169), should change from $a\sqrt{3}$ to $-a\sqrt{3}$. However, solution V should not be discontinuous at a value of $\xi = \pi$, because it is necessary to change its representation, using instead of V_1 the roots V_2 or V_3. In this case, from formulas (172) and (173), we choose root V_2, which changes from $-a\sqrt{3}$ to $a\sqrt{3}$ at $\xi = \pi$, just like $V_3 = 0$ at $\xi = \pi$. Thus, at $\xi = \pi$, solution $V = V_1(\xi)$ changes to $V = V_2(\xi)$, remaining thereby continuous.

This latter representation is correct up to a value of $\xi = \pi + \xi_S$. With an argument of $\xi = \pi + \xi_S$, the solution completes a new jump from a value of $V = V_2(\pi + \xi_S) = a$ to $V = V_1(\pi + \xi_S) = -2a$, corresponding to a jump from point E to point F.

With further increase in the argument to a value of $\xi = 3\pi/2$, solution $V = V_1(\xi)$ achieves a minimum corresponding to point G in Fig. 23:

$$V(3\pi/2) = V_1(3\pi/2) = -\sqrt[3]{0.5 + 0.5\sqrt{1 - 4a^6}} - \sqrt[3]{0.5 - 0.5\sqrt{1 - 4a^6}}. \quad (175)$$

Expression (175) differs from (174) only in sign.

In passing from increasing argument ξ by means of a value of $\xi = 2\pi$, function $\sin\xi$ again changes its sign and root V_1 changes from $-a\sqrt{3}$ to $a\sqrt{3}$. Since the solution should be continuous at $\xi = 2\pi$, it is necessary to describe it not by root $V_1(\xi)$, but by one of the other roots $V_2(\xi)$ or $V_3(\xi)$. From expressions (172) and (173), we find that with the argument ξ, which increases from a value of $\xi = 2\pi$, the roots are $V_2(2\pi) = -a\sqrt{3}$, $V_3(2\pi) = 0$.

Thus, in passing through the value of the argument $\xi = 2\pi$ for maintaining continuity of the solution, it is necessary to replace its representation with $V_1(2\pi - 0) = -a\sqrt{3}$ by $V_2(2\pi + 0) = -a\sqrt{3}$. Note here that use of the root $V_3 = 0$ at the start of movement $\xi = 0$ was an exception related to choosing an initial condition that does not agree with the established oscillation regime. To describe steady-state periodic movement, it is necessary to use a different root and to set $V(2\pi) = V_2(2\pi) = -a\sqrt{3}$.

The next jump occurs at $\xi = 2\pi + \xi_S$, where V changes from $V = V_2(2\pi + \xi_S) = -a$ to $V = V_1(2\pi + \xi_S) = 2a$. This jump has already been described at $\xi = \xi_S$ and, thus, the first period of oscillations $V(\xi)$ has been studied in its entirety.

In analyzing the behavior of the solution in the latter case, $j - \delta \equiv -a^2 < 0$, $0 < 2a^3 < 1$, we supposed that the function describing the wave profile contains discontinuities. The above-discussed compression jumps (from $V = -a$ to $V = 2a$) and expansion jumps (from $V = a$ to $V = -2a$) can occur only in the case when states B or E of the illustrative point are unstable and, in the opposite case, if states C or F of the point are stable.

To analyze the stability, we examine Eq. (162) taking into account the term contained in the derivative, as well as the small parameter Γ:

$$\Gamma dV/d\xi + V^3 - 3a^2V = \sin\xi. \quad (176)$$

Here there are two time scales: slow time ξ and fast time ξ/Γ. For movement along segment BC, the slow time should be frozen, $\xi = \xi_S$, and $\sin\xi_S = 2a^3$. Consequently, Eq. (176) takes the form

$$\Gamma dV/d\xi = -(V + a)^2(V - 2a). \quad (177)$$

To study the stability of point B, it is necessary to set $V = -a + V'$ in (177) and linearize this equation in relation to the small deviation V':

$$\Gamma dV'/d\xi = 3aV'^2. \quad (178)$$

The solution of this equation,

$$V' = \frac{V'(0)}{1 - 3aV'(0)\xi/\Gamma}, \quad (179)$$

shows that any positive initial perturbation $V'(0) > 0$ is an increasing function of fast time and point B is unstable. Leaving point B, the perturbation increases and the system moves in the direction of point C. Equation (177) demonstrates that C is an immobile point, because in it $V = 2a$ and $dV/d\xi = 0$. To study the stability of state C, in (177), we set $V = 2a + V'$. The corresponding linearized equation has the form

$$\Gamma\frac{dV'}{d\xi} = -9a^2V', \qquad V' = V'(0)\exp\left(-9a^2\frac{\xi}{\Gamma}\right), \quad (180)$$

demonstrating stability: any initial perturbation $V'(0)$ fades with an increase in fast time. The instability of

point E and stability of point F, validating the second jump of EF, is proved by an analogous method.

We now construct a resonance curve for induced discontinuous oscillations. An analysis of the frequency characteristic can be performed now by numerical methods with the solutions to Eqs. (176)–(182). Clearly, the resonance curve for discontinuous waves should differ significantly from quasi-linear characteristics calculated by the method of harmonic balance, which are illustrated in Fig. 20.

Here, with the goal of clarifying the main features, we limit ourselves only to a qualitative analysis of the simplified model problem, discussed with the help of Figs. 21–23.

To obtain the analytical formulas, we pass from statement of the problem based on cubic equation (163) with the additional conditions (164),

$$f(V) = V^3 + 3(j-\delta)V = \sin\xi, \quad \langle V\rangle = 0, \quad \langle V^2\rangle = j, \tag{181}$$

to the model statement of the problem:

$$f(V) = V|V| + 2(j-\delta)V = \varphi(\xi), \quad \langle V\rangle = 0, \quad \langle V^2\rangle = j. \tag{182}$$

Here, the cubic parabola is approximated by the two arcs of a quadratic parabola, and the sine in the right-hand side of (181) is replaced by the function

$$\varphi(\xi) = 1-\xi^2, \quad -1<\xi<1; \qquad \varphi(\xi) = -1+(\xi-2)^2, \quad 1<\xi<3, \tag{183}$$

which periodically continues with period 4. Model (182), (183) admits a full analytical solution. We perform an analysis below according to the scheme described above for induced shocked waves; points (1–4) both there and here completely correspond to each other.

1. Let the mean intensity be greater than the detuning, i.e., $j-\delta \equiv a^2 > 0$. Equation (182) for this case in the half-period $-1 < \xi < 1$ takes the form

$$f(V) = V^2 + 2a^2V = 1-\xi^2. \tag{184}$$

Averaging the solution to quadratic equation (184), we find

$$\langle V^2\rangle = j = \delta(a^2) + a^2, \tag{185}$$

where

$$\delta(a^2) = a^4 - a^2 + \frac{2}{3} - a^2(1+a^4)\arcsin(1+a^4)^{-1/2}. \tag{186}$$

2. Let the mean intensity be equal to the detuning, i.e., $j-\delta = 0$. Equation (182) for this case at $-1 < \xi < 1$ has the form

$$f(V) = V^2 = 1-\xi^2. \tag{187}$$

Averaging the solution, we find $\delta = j = 2/3$.

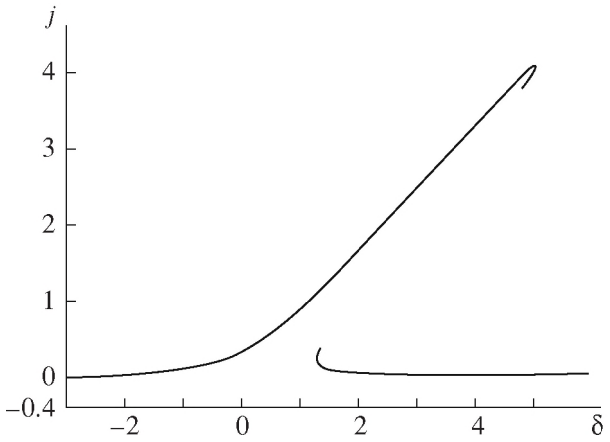

Fig. 24. Resonance curve for discontinuous oscillations in a cubic nonlinear acoustic resonator.

3. Let a positive detuning be greater than the mean intensity, i.e., $j-\delta \equiv -a^2 < 0$ and, in addition, $a^2 > 1$. Equation (182) for this case in the area of $-1 < \xi < 1$ has the form

$$f(V) = V^2 - 2a^2V = 1-\xi^2. \tag{188}$$

Calculation gives the formula

$$\delta(a^2) = a^4 + a^2 - \frac{2}{3} - a^2(a^4-1)\ln\sqrt{\frac{a^2+1}{a^2-1}}. \tag{189}$$

4. Let a positive detuning be greater than the mean intensity, $j-\delta \equiv -a^2 < 0$, but $a^2 < 1$. Averaging of the solution to Eq. (188) taking into account the jumps described in Fig. 23 leads in this case to the expression

$$\delta(a^2) = 3a^4 + a^2 + \sqrt{1-a^4}\left[\frac{2}{3} + \left(\frac{1}{3} + \frac{\sqrt{2}}{2}\right)a^4\right] + \frac{1}{2}a^2(1-a^4)\ln\sqrt{\frac{1-a^2}{1+a^2}} + \frac{1}{2}a^2(1+a^4)\left[\arcsin\sqrt{\frac{1-a^4}{1+a^4}} + \arcsin\frac{1}{\sqrt{1+a^4}}\right]. \tag{190}$$

The three branches of the resonance curve (186), (189), and (190) are continuously sewn together, as is shown in Fig. 24. Comparing the curves in Figs. 24 and 20, we can draw the conclusion that the frequency characteristic in Fig. 24 is the limit curve for the characteristics of Fig. 20 in the case when viscosity tend to zero or the amplitude of boundary oscillations tends to infinity. As well, nonlinear absorption in the shock fronts exceeds the regular linear absorption. As seen in Fig. 24, the intensity of the field in the resonator cannot exceed a certain maximal value; that is, nonlinear saturation takes place.

The ambiguity in the dependence of field intensity on detuning in Fig. 24 is apparently eliminated when a maximum is achieved by fluid increase or decrease in the frequency of wall oscillations, by analogy to induced oscillations in the Duffing equation model. The latter problem is laid out in many textbooks on oscillation theory and is very detailed in [40]. If this analogy is true, for the maximum field intensity to be achieved, the frequency of wall oscillations should increase; after the maximum has been achieved, the intensity decreases jumpwise to a certain small value. If we now decrease the frequency, then the inverse jump from the lower to the higher branch takes place at another, lower, value of detuning δ. Thus, smooth variation of the frequency of wall oscillations at large amplitudes leads to a hysteresis. In the area of the detuning value, where there is a hysteresis, bistability is possible in connection with the described jumps, as well as a transfer from regular to chaotic field oscillations in the resonator. This analogy, however, can seem incorrect, because a resonator is a more complex system that is not described by ordinary differential equations. To check the correctness of the analogy and explain the behavioral features of the resonator as those of a nonlinear distributed system, additional studies are necessary.

REFERENCES

1. O. V. Rudenko and S. I. Soluyan, *Theoretical Foundations of Nonlinear Acoustics* (Nauka, Moscow, 1975; Consultants Bureau, New York, 1977).
2. V. B. Braginskiĭ, V. P. Mitrofanov, and V. I. Panov, *Systems with Small Dissipation* (Nauka, Moscow, 1981; University of Chicago Press, Chicago, 1986).
3. V. P. Mitrofanov, Doctoral Dissertation in Mathematical Physics (Fiz. Fakult. Mosc. Gos. Univ., Moscow, 1996).
4. V. B. Braginsky, V. P. Mitrofanov, and K. V. Tokmakov, Phys. Lett. A **218**, 164 (1996).
5. L. K. Zarembo, O. Yu. Serdobol'skaya, and I. P. Chernobaĭ, Akust. Zh. **18**, 397 (1972) [Sov. Phys. Acoust. **18**, 333 (1972)].
6. R. Landbury, Phys. Today **51** (2), 23 (1998).
7. C. C. Lawrenson, B. Lipkens, T. S. Lucas, et al., J. Acoust. Soc. Am. **102**, 3064 (1997).
8. Y. A. Ilinskii, B. Lipkens, T. S. Lucas, et al., J. Acoust. Soc. Am. **104**, 623 (1998).
9. O. V. Rudenko, Akust. Zh. **29**, 398 (1983) [Sov. Phys. Acoust. **29**, 234 (1983)].
10. O. V. Rudenko, Priroda, No. 7, 16 (1986).
11. V. G. Andreev, V. É. Gusev, A. A. Karabutov, and O. V. Rudenko, Akust. Zh. **31**, 275 (1985) [Sov. Phys. Acoust. **31**, 162 (1985)].
12. V. V. Kaner, O. V. Rudenko, and R. V. Khokhlov, Sov. Phys. Acoust. **23**, 432 (1977).
13. V. V. Kaner and O. V. Rudenko, Mosc. Univ. Phys. Bulletin **33** (1978).
14. M. B. Vinogradova, O. V. Rudenko, and A. P. Sukhorukov, *Wave Theory* (Nauka, Moscow, 1990) [in Russian].
15. O. V. Rudenko and A. V. Shanin, *Nonlinear Phenomena in Structures with Movable Boundaries* (Academic, New York, Goettingen, 1999).
16. O. V. Rudenko and A. V. Shanin, Acoust. Phys. **46**, 334 (2000).
17. A. A. Karabutov and O. V. Rudenko, Sov. Phys. Acoust. **25**, 306 (1980).
18. O. V. Rudenko, JETP Lett. **20**, 203 (1974).
19. A. A. Karabutov, E. A. Lapshin, and O. V. Rudenko, Sov. Phys. JETP **44**, 58 (1976).
20. M. J. O. Strutt, *Lame, Mathieu and Related Functions in Physics and Technology* (Edwards Brothers, New York, 1944).
21. O. V. Rudenko, K. M. Hedberg, and B. O. Énflo, Akust. Zh. **47**, 525 (2001) [Acoust. Phys. **47**, 452 (2001)].
22. B. O. Enflo, C. M. Hedberg, and O. V. Rudenko, J. Acoust. Soc. Am. **117**, 601 (2005).
23. M. Abramovitz and I. A. Stegun, *Handbook of Mathematical Functions* (Dover, New York, 1970).
24. W. Chester, J. Fluid Mech. **18**, 44 (1964).
25. O. V. Rudenko, A. L. Sobisevich, L. E. Sobisevich, and K. M. Hedberg, Dokl. Akad. Nauk, Ser. Fiz. **383**, 330 (2002).
26. M. Van Dyke, *Perturbation Methods in Fluid Mechanics* (Parabolic, Stanford, CA, 1975).
27. O. V. Rudenko, Dokl. Akad. Nauk **360**, 759 (1998) [Dokl. Phys. **43**, 346 (1998)].
28. O. V. Rudenko, Akust. Zh. **45**, 397 (1999) [Acoust. Phys. **45**, 351 (1999)].
29. O. V. Rudenko, Akust. Zh. **44**, 786 (1998) [Acoust. Phys. **44**, 684 (1998)].
30. I. P. Lee-Bapty and D. G. Crighton, Philos. Trans. Roy. Soc. London A **323**, 173 (1987).
31. O. V. Rudenko and O. A. Sapozhnikov, Zh. Éksp. Teor. Fiz. **106**, 395 (1994) [JETP **79**, 220 (1994)].
32. A. P. Sarvazyan, O. V. Rudenko, S. D. Swanson, et al., Ultrasound Med. Biol. **24**, 1419 (1998).
33. S. Catheline, J.-L. Gennisson, and M. Fink, J. Acoust. Soc. Am. **114**, 3087 (2003).
34. V. G. Andreev and T. A. Burlakova, Acoust. Phys. **53**, 44 (2007).
35. L. A. Ostrovsky and P. A. Johnson, Riv. Nuovo Cim. **24**, 1 (2001).
36. O. V. Rudenko, Usp. Fiz. Nauk **165**, 1011 (1995) [Phys. Usp. **38**, 965 (1995)].
37. O. V. Rudenko and O. A. Sapozhnikov, Usp. Fiz. Nauk **174**, 973 (2004) [Phys. Usp. **47**, 907 (2004)].
38. B. O. Enflo, C. M. Hedberg, and O. V. Rudenko, AIP Conf. Proc. **834**, 187 (2006).
39. O. V. Rudenko, K. M. Hedberg, and B. O. Énflo, Akust. Zh. **53**, 522 (2007) [Acoust. Phys. **53**, 455 (2007)].
40. A. P. Kuznetsov, S. P. Kuznetsov, and N. M. Ryskin, *Nonlinear Oscillations* (Fizmatlit, Moscow, 2002) [in Russian].

Translated by A. Carpenter